5-27-1968

Pressure and Temperature Dependence of the Acoustic Velocities in Polymethylmethacrylate

James Russell Asay

ACOUSTIC VELOCITIES IN POLYMETHYLMETHACRYLATE - ASAY

This thesis, directed and approved by the candidate's committee, has been accepted by the Graduate Committee of The University of New Mexico in partial fulfillment of the requirements for the degree of

Master of Science in Physics

PRESSURE AND TEMPERATURE DEPENDENCE OF THE ACOUSTIC VELOCITIES IN POLYMETHYLMETHACRYLATE

Title

James Russell Asay

Candidate

Physics

Department

Dean

5-27-68

Date

Committee

Chairman

PRESSURE AND TEMPERATURE DEPENDENCE OF THE ACOUSTIC VELOCITIES IN POLYMETHYLMETHACRYLATE

BY
JAMES RUSSELL ASAY
B.A., San Jose State College, 1964

THESIS

Submitted in Partial Fulfillment of the
Requirements for the Degree of
Master of Science in Physics
in the Graduate School of
The University of New Mexico
Albuquerque, New Mexico
June 1968

ACKNOWLEDGMENTS

The author wishes to acknowledge his debt of gratitude to his Research Supervisor, Professor John R. Green, for for his guidance and support during the course of this research. Acknowledgment and sincere thanks are likewise due to his Research Advisor, Dr. Arthur H. Guenther of Kirtland Air Force Base who, for the last four years, has provided invaluable assistance in the techniques and approaches involved in experimentation and data reduction.

The author is deeply grateful to Major Donald L. Lamberson who assisted in the operation of the pressure equipment and for valuable discussions relating to the experiment.

Finally, the author would like to express his thanks to Mr. I. S. Smith for the maintenance of the pressure system and to the many others who have made this research possible.

PRESSURE AND TEMPERATURE DEPENDENCE OF THE ACOUSTIC VELOCITIES IN POLYMETHYLMETHACRYLATE

BY

James Russell Asay

ABSTRACT OF THESIS

Submitted in Partial Fulfillment of the
Requirements for the Degree of
Master of Science in Physics
in the Graduate School of
The University of New Mexico
Albuquerque, New Mexico
June 1968

ABSTRACT

The acoustic velocities in polymethylmethacrylate have been measured with an ultrasonic pulse echo technique as functions of frequency, temperature and pressure. At atmospheric pressure, data on the velocities and attenuation coefficients were obtained over the range of temperature from 22°C to 75°C and for the frequency range of 6 to 30 MHz. At the temperatures of 25, 40, 55 and 75°C, the pressure dependence of the longitudinal and shear velocity was obtained to 150,000 psi at a frequency of 6 MHz. From the frequency measurements of the velocities, the complex elastic moduli in polymethylmethacrylate were calculated at room temperature. The pressure dependence of the velocities allowed the determination of the elastic constants as a function of pressure. It was found that the measured velocities for increasing pressure were generally lower than those for decreasing pressure by about 0.5% for the longitudinal measurements and about 0.8% for the shear measurements. However, the acoustic measurements of the velocities at atmospheric pressure after the specimens had been exposed to 150,000 psi were usually within 0.1% of the initial values. After exposure to pressure the lengths of the specimens also reproduced the initial measurements to

within 0.05%. A discussion is presented which illustrates some of the applications of the data reported here with respect to equation of state determinations in polymeric materials at elevated pressures.

TABLE OF CONTENTS

LIST OF FIGURES

Figure Page

LIST OF TABLES

ABBREVIATIONS AND SYMBOLS

Hz	Cycles per second. MHz = Megacycles per second.
V	Velocity. The quantities V_ℓ and V_t refer to the longitudinal and shear velocities, respectively.
ρ	Density, g/cm^3.
Z	Mechanical impedance, defined as ρV. The units are mech. $ohms/cm^2$ (1 mech. ohm/cm^2 = 1 gm/cm^2 sec).
f	Acoustic frequency.
φ	Phase shift for acoustic reflection from a boundary.
λ	Lame' constant relating to longitudinal wave propagation.
μ	Lame' constant governing shear wave propagation. Identical with the shear modulus G.
E	Young's modulus.
σ	Poisson's ratio.
B	Bulk modulus, defined thermodynamically as $B = - v(\frac{\partial P}{\partial v})$, where v is the volume and P is the pressure. For this and the other moduli, a superscript S or T refers to the adiabatic or isothermal modulus, respectively.
ϵ	Strain.
k	Propagation constant.
α	Attenuation coefficient for plane wave propagation.

β Volume coefficient of expansion. Approximated as three times the linear expansion coefficient for amorphous polymers.

γ Grüneisen ratio, defined thermodynamically as

$$\gamma = \frac{\beta B^{s}}{\rho c_{p}} \quad .$$

c_p Specific heat at constant pressure.

SECTION I

INTRODUCTION

This research was performed at Kirtland Air Force Base as part of a continuing effort to describe the behavior of materials exposed to extreme temperature and pressure conditions. The particular technique presented here involves the ultrasonic determination of the acoustic velocities in solids as a function of temperature and, more importantly, as a function of pressure. Through the conventional equations of elasticity, the pressure and temperature derivatives of the elastic moduli can then be determined.

As recently illustrated by Anderson[1] (1), the pressure dependence of the bulk modulus can be used in the Murnaghan equation (21) to define semi-emperically the equation of state of solids at various temperatures, so that in principle the PVT surface can be mapped out. As Anderson emphasizes, the pressure-volume relation thus obtained is not necessarily confined to the pressure range over which the measurements are obtained, but can be extrapolated to pressures orders of magnitude higher, in some instances. For a wide variety of

---

[1]The numbers in parentheses refer to references at the end of the text.

single crystals and for some polycrystalline materials, he has shown that the equation of state estimated in this way agrees reasonably well with experimental high pressure measurements, such as those obtained through dynamic techniques, providing that the material does not undergo any phase changes over the region of extrapolation.

In a theoretical sense, the agreement between the estimated equation of state as obtained through the ultrasonic approach and that obtained directly with the high pressure shock techniques (after suitable corrections have been applied) tends to support the Murnaghan equation as a reliable equation of state for a wide variety of materials. More practically, however, the ultrasonic technique allows a rapid and convenient estimation of the high pressure equation of state without recourse to the time consuming and expensive shock wave analyses.

Since the ultrasonic pressure technique had not been previously available at Kirtland, one of the major objectives of the present research was to assemble the necessary pressure and electronic equipment prerequisite to the precise determinations of acoustic velocities at high pressure. The second objective was to determine the pressure and temperature derivatives of the acoustic

velocities in a typical plastic over the pressure and temperature ranges of ambient to about 150,000 psi and from 25 to 75°, respectively. Since Anderson's approach has not heretofore been applied to plastics, the present research allows a comparison of his extrapolation technique in the estimation of the high pressure equation of state of polymeric materials.

SECTION II

EXPERIMENTAL METHOD

1. Ultrasonic Velocity Techniques

The emphasis in the present research was to establish a technique for determining velocity and velocity changes as accurately as possible. Although there are numerous techniques illustrated in the literature which accomplish this purpose, the materials which generally have been analyzed have exhibited low acoustic absorption so that high frequency pulse reflection or resonant techniques have been applicable. These techniques generally rely upon the superposition of the acoustic signals with a suitable reference signal so that accuracies of 10^{-5} to 10^{-8} have, in some instances, been obtained (5, 17).

In plastics, however, the acoustic absorption for either shear or longitudinal waves in the megacycle range is too high in most cases to apply some of the more conventional techniques of measuring sound velocities. The difficulty is further compounded by the fact that the acoustic velocities in this frequency range are generally dispersive. Considering these problems, the author decided to establish a technique for determining acoustic velocities in the frequency range of ~6-30 MHz with an uncertainty of 0.1 percent or less in the velocities.

Two different methods were found to satisfy these requirements. The first was developed approximately ten years ago by Williams and Lamb (27) and, although it has not been extensively used, it offers the advantage of relatively high accuracy in moderately absorbing materials.

The experimental technique is illustrated schematically in Figure 1. A General Radio 1330A[1] continuous wave oscillator drives an Arenberg 650C pulsed amplifier.[2] The pulsed amplifier incorporates a gating circuit which allows the amplification of the input CW signal into two phase-coherent RF pulses for every repetition of the amplifier. The RF output pulses are essentially flat-topped with rise and fall times of about one-half microsecond (μsec), pulse lengths ranging from one to 20 μsec with variable carrier frequencies in the range of ~0.2-180 megacycles/sec (MHz) and peak to peak amplitudes of up to 500 volts.

The RF pulse is applied through a 93 ohm coaxial cable to one of two closely matched transducers located on flat and parallel surfaces of the specimen. The transmitting transducer excites acoustic vibrations which are received by the second crystal, amplified[3] and

---

[1]General Radio Corp., Cambridge, Mass.

[2]Arenberg Ultrasonic Laboratory, Jamaica Plains, N.Y.

[3]Arenberg Wide Band Amplifier, Model WA-600B.

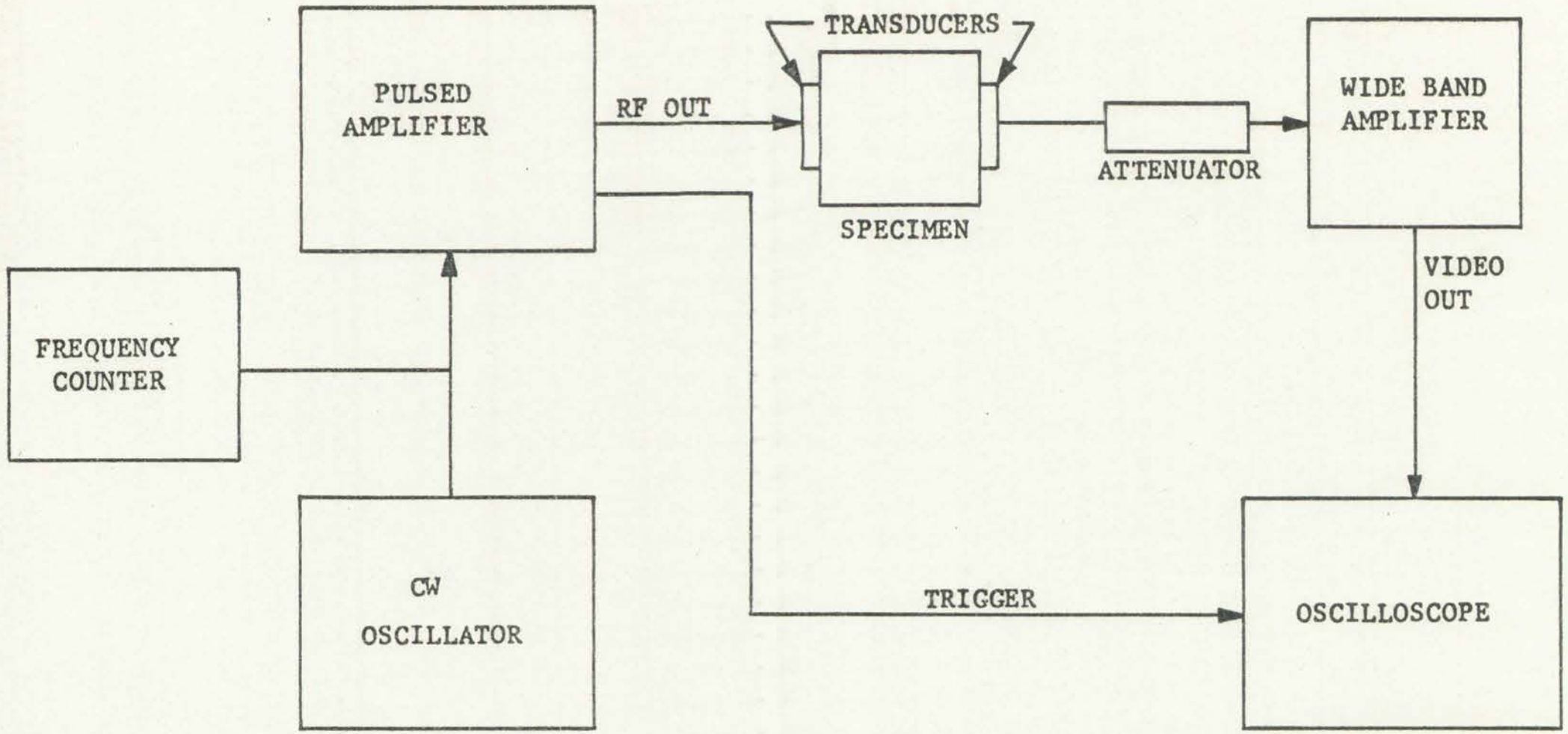

Figure 1. Schematic Diagram of the Williams and Lamb Technique for Determining Acoustic Velocities

displayed on the oscilloscope.[1] A 93 ohm attenuator[2] is used to compare the amplitude of the acoustic signal which has traversed one length of the specimen with one or more of the echoes resulting from that signal.

In the resulting technique the RF pulses are obtained by gating and amplifying the output of the continuously running oscillator. The sinusoidal frequency in the pulse can therefore be measured to a high degree of accuracy. As illustrated in Figure 1, a frequency counter[3] was used to determine the RF frequency to within one part in 10^6.

The pulsed amplifier is tuned to the CW frequency input of the oscillator by inserting various frequency range inductance coils and capacitatively tuning the RF output to a maximum. The advantage of this amplifier over most conventional pulsed amplifiers is that a double pulse output can be obtained for each repetition of the amplifier. The second pulse is phase coherent with the first, its amplitude is independently controlled, and its delay time and pulse width can be continuously varied with respect to the first pulse. When the oscillator was first received, the minimum time that the second pulse could be delayed with respect

---

[1] Tektronix, Model 555.

[2] Arenberg, Model ATT-693.

[3] Hewlett Packard, Model 5245L.

to the first was 20 μsec. Since the delay time must approximate twice the transit time in the specimen and since the attenuation in plastics is rather high in the megacycle region, it was necessary to maintain relatively low transit times so that the minimum delay was modified to ~ 7 μsec.

Figure 2 illustrates the application of this technique (hereafter referred to as the Williams and Lamb Technique) to the determination of either the longitudinal or shear velocity in a solid specimen. Two closely matched transducers (i.e., transducers with nearly identical physical dimensions and with resonant frequencies within 1 percent of each other) are placed on each of the two flat and parallel surfaces of the specimen. The pulsed amplifier is then triggered internally at a rate of about one kilocycle per second, and for each repetition, two RF pulses are applied to one of the transducers. The carrier frequency in the pulse is adjusted to the resonant frequency of the transducer so that acoustic pulses of approximately the same time duration are excited in the specimen. The signals thus received on the second transducer are amplified and the rectified output displayed on the oscilloscope. As shown in the figure, the first acoustic pulse generates a series of signals on the

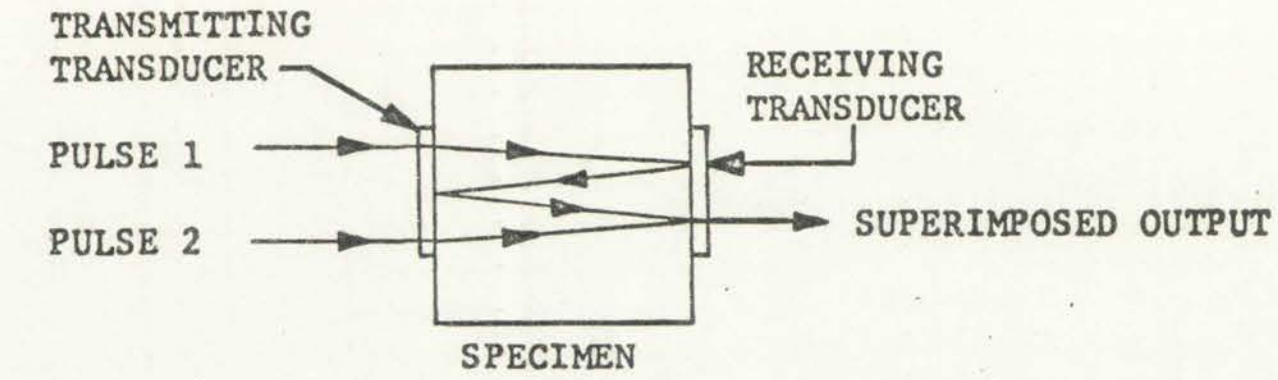

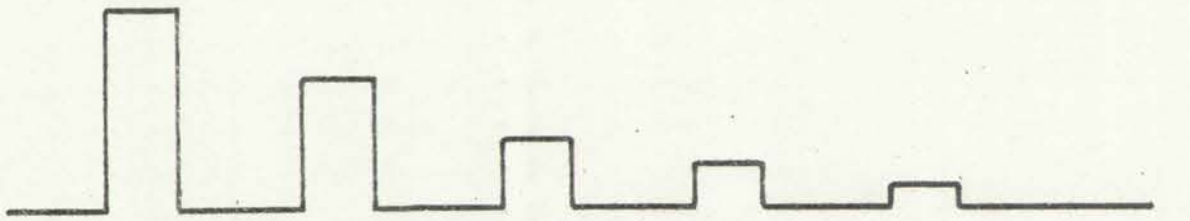

(1) ECHO TRAIN OF PULSE 1

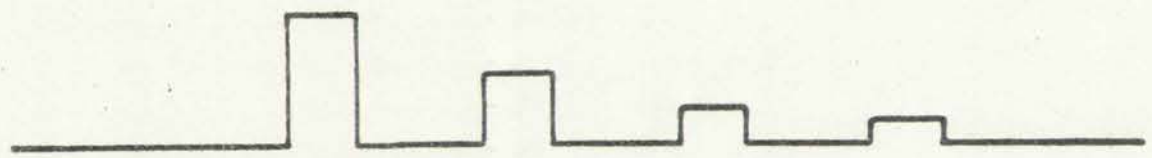

(2) ECHO TRAIN OF PULSE 2

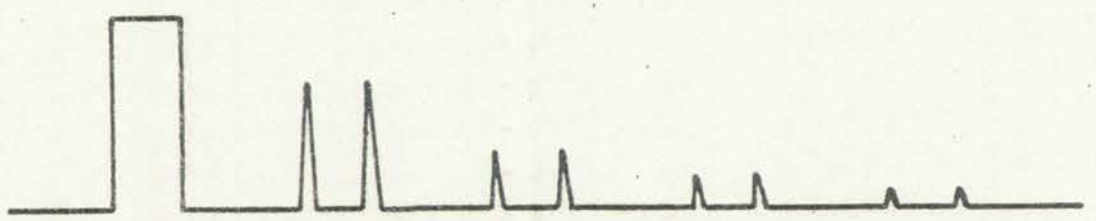

(3) CANCELLATION DUE TO ADDITION OF (1) AND (2)

Figure 2. Illustration of the Method of Superimposing the Echoes with the Williams and Lamb Technique

second transducer, which correspond to the first transmitted signal and the corresponding echoes which result from reverberation of the pulse within the specimen. The second applied signal generates a similar wave train on the receiving transducer. The amplitude of the second applied pulse is now adjusted so that the amplitude of the straight transmitted signal is equal to that of the first echo from the first pulse. By adjusting the delay of the second pulse, we can make these two signals overlap and cancel for particular values of the carrier frequency.

In practice, it was found that the highest sensitivity was obtained with relatively large pulse widths and with the maximum gain on the wide band amplifier. The maximum pulse widths of the applied signals (which are generally approximately equal) are limited to twice the transit time through the specimen in order to avoid overlap of the echoes in either wave train. Normally, the widths were approximately 5-10 μsec in duration.

As shown in Figure 2, complete cancellation of the two signals was seldom achieved. That is, generally there were residue signals left at the beginning and end of the cancelled peaks in the superimposed output. These residues are caused by differences in pulse widths and rise times and transients in the applied pulse. However,

this effect does not influence the velocity calculations, since superposition is generally obtained for the middle portions of the pulse.

For some of the thicker specimens analyzed in the present experiment at the higher frequencies, the first received echo was only a few db above the background CW signal leaking through the chassis. Although this CW leakage is 40-60 db below the output pulse, a modulation effect is observed when a weak signal is superimposed on this background and the RF frequency is varied. This effect was reduced by mounting a pair of back-to-back diodes (1N67A) at the RF output. With this arrangement, echoes as low as 50 db below the transmitted pulse could be studied without modulation with the background.

Some of the advantages and disadvantages of this technique are discussed in Appendix I. It is shown there that accuracies of 1 part in 10^4 can be achieved with the method if proper account is taken of the phase shift coefficient for reflection at the transducer-specimen boundary. This effect arises because the transducers are attached to the sample with a thin layer of oil or some other bond (see the next section).

This method has not been used extensively in the literature for determining changes in the velocity. In

the present report it is shown that the technique is extremely useful for determining small velocity changes with pressure and temperature in materials which are moderately absorbing. For the present range of RF frequencies and sample thicknesses utilized in this study, changes in the null frequencies of one part in 10^4 could be observed for a given environmental change. If other parameters, such as the variation in the bond characteristics and the shift in the resonant frequency of the transducer are known, a change in the velocity of two or three parts in 10^4 can easily be detected.

It is also shown in Appendix I that the absolute value of the phase shift coefficient pertaining to acoustic reflection at the transducer boundary is unity. This results from the fact that the effective mechanical impedance of the bond and transducer, as seen from the specimen, is purely reactive. Therefore, this technique allows the determination of the wave attenuation by measuring the amplitudes of successive echoes in the wave train. As shown in Figure 1, an attenuator was used to measure echo amplitudes. The attenuator used here was a 93 ohm step attenuator with a maximum range of 122 db, variable in 1 db increments. It had previously been calibrated by the manufacturer to ±1 db. The attenuation of the echoes within the specimen was obtained by

inserting attenuation for each echo so as to match its amplitude to a given voltage signal on the oscilloscope. The attenuation of the wave in the specimen could then be obtained by averaging the results of three to four echoes. Although the amplitude difference from one echo to the next could only be determined to ±1 db, the accuracy could be somewhat improved by measuring the attenuation in this way for a number of different specimens. Systematic errors can then be determined by performing a linear least-squares analysis of attenuation as a function of sample thickness.

The other technique used in the present study for determining velocities has been described in an earlier paper (2). Basically, the approach is essentially the same as the Williams and Lamb technique and is schematically outlined in Figure 3. Now, however, the Arenberg pulsed amplifier is converted into a pulsed oscillator (i.e., an oscillator tube is excited externally for every repetition of an applied trigger), which is triggered at a 10 kilocycle rate by a time mark generator.[1] The time mark generator simultaneously triggers a Tektronix 555 dual beam oscilloscope and displays 1 μsec time marks[2] on one beam of the oscilloscope. As shown in the figure, the single RF pulse which is generated for every

---

[1] Tektronix 180A.

[2] These marks were calibrated to an accuracy of 1 part in 10^6.

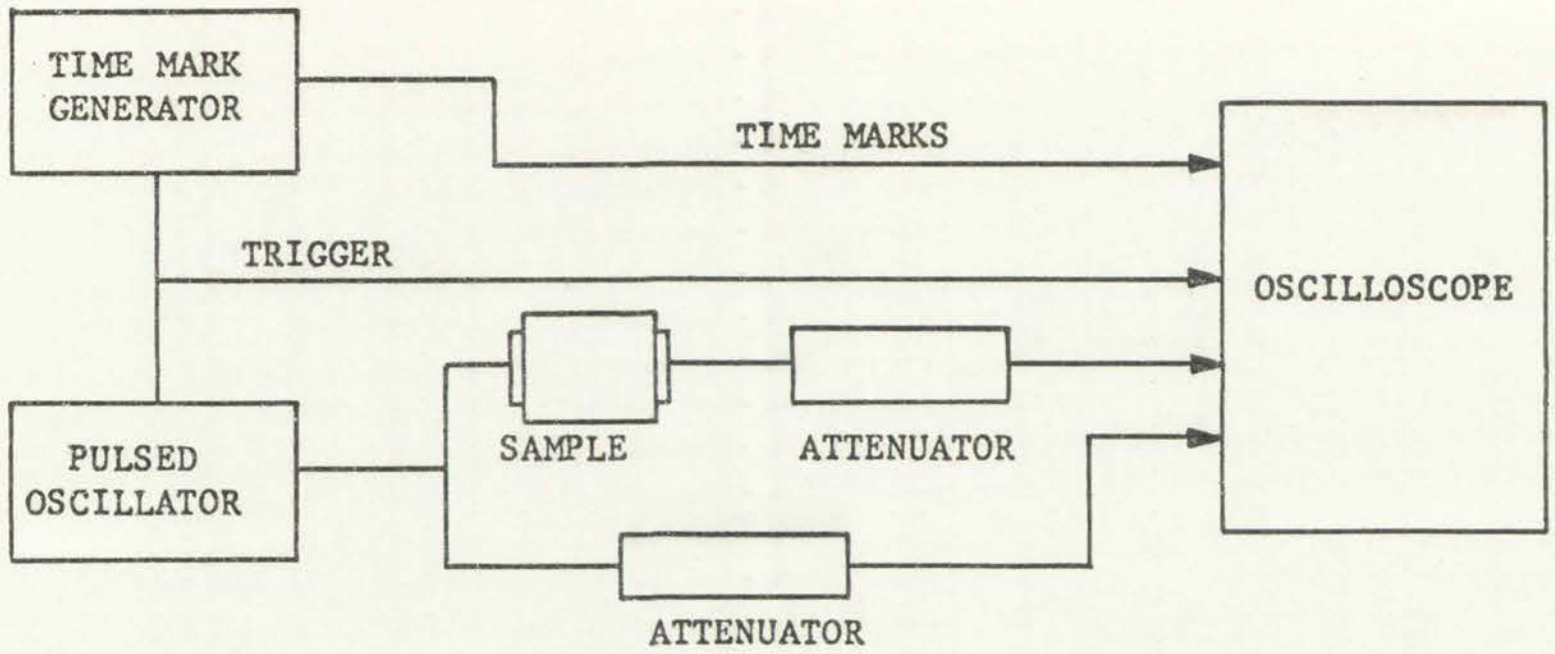

Figure 3. Illustration of the Transmission Technique for Determining Relative Changes in Acoustic Velocities

repetition is then applied to the transmitting transducer and displayed on one trace of the other beam. The received acoustic signal is amplified[3], if necessary, and displayed on the other trace. The attenuators are used to prevent overloading the oscilloscope.

The transit time for the direct transmitted signal is determined by displaying the unrectified wave forms of the transmitted and received signals on the oscilloscope and using the calibrated delay sweep potentiometer of the oscilloscope to identify two corresponding peaks near the middle of the respective pulses as references. The transit time is then determined by counting the number of time marks between the two reference peaks and by linearly interpolating the times of the reference peaks between marks. That is, the time marks on either side of the desired reference peak, and the peak itself, are successively aligned on some vertical grid line of the oscilloscope display and the corresponding readings on the delay potentiometer noted. The time between one time mark and the reference peak is then obtained by linear interpolation. This technique requires the assumption that the delay circuit is sufficiently linear over any 1 μsec interval that linear interpolation applies. To ensure that the delay was sufficiently linear,

---

[3]An amplifier is not shown in Figure 3. However, if amplification is necessary, the amplifier is inserted on the receiving branch between the attenuator and the oscilloscope.

calibrated 5 and 10 MHz sine waves were simultaneously displayed on the oscilloscope with the 1 μsec time marks and delay readings taken of the peaks in the sine wave and of the 1 μsec marks. By comparing the readings of each set it was determined that the delay was sufficiently linear to justify the interpolation method.

This technique was not used for any absolute velocity measurements because it is relatively difficult to accurately determine the phase shifts in the amplifier and the oscilloscope, or the acoustic delays in the transducer bonds. However, since time differences of the order of 0.004 μsec can be reliably determined, the approach is attractive for velocity measurements. The method was used for some of the pressure and temperature measurements where at least one echo could not be obtained. This effect occurred for some of the higher temperature isotherms and at some of the higher pressures where deterioration of the bond prevented well-separated acoustic signals.

The main disadvantage of the technique for precision measurements of velocity changes results from the change in the bond characteristics for a given environmental change. For the temperature measurements, the temperature coefficient of velocity in some of the bonds used in the experiment was known, so that the correction to the

transit time could be determined if the bond thickness remained relatively constant. However, for the pressure determinations, very little is reported in the literature regarding density and velocity variations for the more common bonding materials. McSkimin (17) indicates that the velocity of a common bond material, Nonaq stopcock grease, approximately doubles over the pressure range employed here.

The transducers are normally bonded to the specimen with a bond thickness on the order of 1 micron (see Appendix I). If the transit time error is given by the bond thickness divided by the acoustic velocity in the bond, a value of ~ 0.001 μsec results for longitudinal waves traversing a light oil bond. If the velocity in the oil doubles at the highest pressures obtained in the present experiments, the resulting correction that should be applied with respect to the error at atmospheric pressure is ~ -0.0015 μsec per bond. For all of the measurements with pressure obtained by this method, the resulting error in the relative velocity is on the order of 0.03 percent, which approaches the inherent limitations of the technique. In general, the agreement between the results obtained in this way and those determined by the Williams and Lamb technique agreed to approximately 0.2 percent.

The significant advantage of the Williams and Lamb technique over the transmission technique is that the phase changes occurring at the transducer boundary are relatively negligible for different pressures and temperature conditions, if the bonds are thin. This results from the fact that the bond presents a mass loading to the specimen at the resonant frequency which is essentially independent of pressure changes (see Appendix I). The equivalent mechanical impedance of the transducer-bond combination is then a small function of pressure, so that the phase angle for waves reflected at this boundary remains practically constant. This effect will be discussed in more detail in Section III.

2. Sample Preparation

The polymethylmethacrylate (PMMA) material used in the present experiment was obtained from the Cadillac Plastic Company as 2-1/2 inch diameter cast rod.[1] The rod was turned on a lathe to a diameter of 1.1 inch and then milled into samples of various thicknesses. With this technique, the resulting specimens exhibited flatness on the order of 3-10 microns and parallelism of about two minutes of arc. Samples exceeding these limits were discarded. The samples were then lightly polished by

---

[1] Cadillac Plastic & Chemical Co., Detroit, Michigan. Acrylux rod, liquo-temp annealed, ASTM D-788-56, Grade 5.

hand on a lapping wheel successively with wet number 600 coarse and 600 fine sandpapers to remove any machining marks.[1] The resulting polished specimens were optically transparent with approximately the initial physical dimensions.

The thicknesses of the specimens used in the experiment were obtained after polishing and ranged from about 3 to 14 mm. This range was chosen in order to identify and correct any systematic errors in the velocity or attenuation results. In addition, the attenuation per unit length at the higher frequencies significantly restricted specimen thicknesses, particularly in the case of shear waves where the attenuation is approximately twice that for longitudinal propagation.

The density of the material analyzed here was obtained by weighing the specimens and calculating the volume through the use of the physical dimensions. The average density of all the specimens analyzed, as determined in this way, was 1.180 ± 0.001 gm/cm^3.

---

[1]For some of the pressure measurements of the velocities, better results were obtained by using the specimens without fine polishing. It was found that internal or surface strains were normally induced in the samples through the polishing procedure, as easily observed by placing the specimen between crossed polaroids. The propagation velocities did not appear to be dependent upon the fine polishing. However, it was found that attenuation measurements were affected, since the amplitude of the received longitudinal echoes was increased about 1 db for a finely polished surface.

The samples were then ready for the acoustic measurements. The sample surfaces were prepared by cleaning lightly with acetone and then alcohol. A suitable bonding film was applied to the prepared surfaces so that the transducers could be bonded to the flat surfaces of the specimen.

During the course of the experiment, it was noted that the longitudinal velocity decreased by ~ 0.15 percent after the specimen had been exposed to temperatures of ~ 62°C or higher. This magnitude of variation is well within the limits of error of the Williams and Lamb technique. For this reason, the specimens which were used in the isothermal pressure runs were heated to 80°C for approximately 16 hours and slowly cooled. This was done to separate hysteresis effects due to the simultaneous application of pressure and temperature, thus making it possible to attribute any observed irreversibility to one or the other parameter. Some pressure runs were performed on unheated samples; however, the results will be discussed in Section III.

3. Transducers and Bond Materials

The transducers used for the velocity measurements were obtained commercially.[1] For the longitudinal

---

[1] Valpey Crystal Corp., Holliston, Mass.

measurements 3/4 inch diameter X-cut quartz crystals were employed. These crystals were vacuum plated with a thin chrome-gold deposit so as to provide symmetrical coaxial electrodes. That is, the crystal was completely coated except for a ring approximately 5/8 inch in diameter with respect to the axis of the cylindrical disk and about 1/16 inch wide. The center portion was used as the active center of the transducer and the outer plating was connected to ground.

For the shear measurements AC-cut quartz crystals were used. Although Y-cut quartz or some of the transversely polarized ceramics produce a larger amplitude shear wave for a given electrical input, a quasi-longitudinal mode is usually generated in these crystals which interferes with the shear velocity measurements since the longitudinal velocity is about twice that of the shear velocity. AC-cut quartz vibrates in an almost pure shear mode so that the parasitic longitudinal wave is about 50 db lower than the shear wave if the crystal is properly bonded to the specimen. The AC-cut crystals were likewise coaxially plated with the physical dimensions given above.

The transducers were fine ground finished to a flatness of 0.00005 inch and parallel to less than 15 seconds of arc. Although these specifications prohibited

operation at the extremely high harmonics, the third harmonic could usually be generated and detected fairly easily. Generally, however, the transducers were operated in their fundamental modes. For the measurements reported herein, fundamental frequencies of 6, 10, and 20 MHz were available for both the shear and longitudinal transducers. The results at 18 and 30 MHz presented in the next section were obtained as harmonics.

The resonant frequencies of the transducers were known to within 1 percent. As shown in Appendix I, the exact value of the resonant frequency of the transducer is a necessary prerequisite to obtain the high accuracies possible with the Williams and Lamb technique. Furthermore, it is necessary to match the resonant frequencies of the transmitting and receiving transducers as close as possible. This is necessitated by the fact that the phase shift coefficient for acoustic reflection at the transducer boundary is a function of frequency (see Appendix I). Although a 1 percent variation in the resonant frequency could result in an error of about 0.2 percent for the nominal sample thicknesses employed here (the magnitude of the error depends upon the transit time in the specimen), this effect was checked by using the same transducers on a number of different samples.

A number of various bonds were studied in the present experiment. For the longitudinal measurements, the physical requirements of a bonding material are not generally difficult to meet, since only longitudinal vibrations must be transmitted at boundaries. For the temperature measurements at atmospheric pressure, a light silicone fluid[1] ($Z = 1.205 \times 10^5$ mech. ohms/cm^2) was found satisfactory for the longitudinal measurements.

For the shear measurements the requirements of a bond stiffness are increased, since transverse vibrations must be transmitted at boundaries. In general, the rigid bonds necessary in this case are applicable to only certain ranges of pressure and temperature. For the room temperature measurements at atmospheric pressure, a polystyrene fluid[2] ($Z = 0.9 \times 10^5$ mech. ohms/cm^2) was satisfactory with respect to shear transmission. A very thin bond could be obtained with this material by heating the sample and fluid to about 70°C and then "wringing" the transducer on. However, the material becomes too fluid at 30 or 40°C to transmit shear and therefore could not be used for the temperature measurements at atmospheric pressure.

Several epoxy based adhesives were found satisfactory for the shear wave measurements with temperature at

---

[1]Dow Corning Corp., 220 fluid, Midland, Mich.

[2]Dow Chemical Co., Resin 276-V9.

atmospheric pressure. However, none of these bonds were suitable for the pressure runs. It was found that generally the rigid epoxy bonds would fail at some pressure with the effect that shear wave transmission could not be re-established, even at the lower pressures. This effect was thought to be due to the rather large differences in the linear compressibilities of the quartz and specimen (about 0.0027 $kbar^{-1}$ and 0.017 $kbar^{-1}$, respectively). In some cases, the transducer would be cracked when the sample assembly was removed from the pressure vessel.

The first bond to be tried with the shear wave-pressure measurements was Eccobond 104,[1] which is a high temperature epoxide adhesive with a shear strength of ~ 2000 psi at 150°C. The transducer-bond-specimen was cured at 75°C for about eight hours under slight pressure (~ 5 psi). However, this bond failed irreversibly at 10,000 psi and 25°C.

Another bond which gave somewhat better results for the pressure measurements was a strain gage adhesive,[2] GA-1. This material is a fast-setting resin which requires only a few minutes to cure. This bond failed at 40,000 psi at room temperature.

---

[1]Emerson & Cuming, Inc., Canton, Mass.

[2]Budd Co., Phoenixville, Pennsylvania.

Two other rigid bonds were tried. One was a rubber-based cement[1] which sets up in about 15 minutes. The other was a high-temperature ceramic cement[2] which sets by chemical reaction. Neither of these gave satisfactory results. The rubber-based compound did not allow shear transmission at any pressure. The ceramic cement allowed relatively poor shear transmission to about 20,000 psi, but the transducer was cracked upon removal from the system.

In some of the early pressure runs on the shear velocity, the polystyrene fluid described earlier was used as a bond. However, at room temperature this bond becomes so viscous at the higher pressures that the effect described earlier occurs. That is, the signal abruptly disappeared as the pressure was increased. On the first shear run with this bond, the signal completely disappeared at ~ 125 Kpsi. Relatively good shear transmission was re-established by heating the sample to ~ 75°C while maintaining the pressure at 125 Kpsi. The pressure was then increased to ~ 150 Kpsi with good results. When the pressure was released, the signal amplitude displayed jumps at various pressures. When the specimen assembly was removed, it was observed that the transducer was cracked into three or four major pieces. Furthermore, it

---

[1]Silastic 732 RTV, Dow Corning Corp., Midland, Mich.

[2]Kern Ceram Cement, Kern Chemical Corp., Los Angeles, Calif.

was noticed that voids had formed over part of the surface of the transducer. As a general rule, the detected acoustic wave exhibits a large tail when this sort of effect occurs, so that the received echoes are not well-separated.

The bond that was found best for shear transmission under pressure in PMMA is a thermoplastic consisting of phthalic anhydride and glycerin. A 1:1 mixture of the above constituents was used successively by Renard (23) and Yarnell (28) on the relatively compressible ammonium halides. A 1:1 mixture of this material was made in the present study by heating glycerin and phthalic anhydride together at 135°C for five hours. The resulting compound has about the same viscosity as the polystyrene fluid. With this bond, shear transmission remained good to about 140 Kpsi at 25°C. When the degree of polymerization, and hence the viscosity, was decreased by increasing the relative amount of glycerin, shear transmission was maintained to 150 Kpsi. For the higher temperature isotherms the viscosity was increased by decreasing the relative amount of glycerin. The mixtures which were found most suitable for shear transmission in the present study were 7:4 for 25-40°C and 1:2 for 40-75°C of glycerin to phthalic anhydride, respectively.

This bond was likewise found to provide good longitudinal transmission with pressure and was therefore used

for most of the longitudinal measurements reported herein. Since viscosity was relatively unimportant for the longitudinal measurements, a mixture of 4:1 of glycerin to phthalic anhydride was used for all of the pressure runs.

4. Temperature and Pressure Equipment

The acoustic velocities were first determined at atmospheric pressure and room temperature. For the room temperature measurements, the acoustic assembly was immersed in a constant temperature lab bath with a control temperature of better than 0.2°C. A thermometer which had previously been calibrated to 0.2°C was used to measure the temperature of the bath. For these measurements, the specimen was immersed in the bath for a minimum of one hour before velocity measurements were made.

The two transducers mounted on the specimen were shielded from each other by aluminum holders which completely covered the free surface of the crystals and provided ground contact to the outer portion of the coaxial plating on the transducer. A spring-loaded electrode in the holder allowed electrical contact to the active center of the transducer.

The pressure equipment was obtained commercially from Harwood Engineering Company.[1] The generating system

[1]Harwood Engineering Co., Walpole, Mass.

and pressure vessel are shown schematically in Figure 4. The heart of the system consists of two single-acting intensifiers[1] which are hydraulically driven. The first intensifier operates on an intensifier ratio of 28.5:1 from a gas intake of 1-2000 psi and maximum output of 50 Kpsi. The second intensifier possesses a 130:1 hydraulic advantage with a minimum intake of ~ 2000 psi and a maximum high pressure of 200 Kpsi.

In the present experiment argon gas, at an initial pressure of ~ 2000 psi, was used as the high pressure fluid. The generation of pressure in the vessel is obtained as follows: The valves X-1 through X-3 are opened and equilibrium is established with the argon supply. The second intensifier is put in the return stroke position with the four-way value B. The value X-1 is closed and the first intensifier is brought to the top of its stroke with the four-way valve A and the valve X-2 is closed. The first intensifier is then fully retracted, another charge of gas is admitted, X-1 is closed and the pressure in I-1 is increased until it reaches the pressure in the rest of the system. X-2 is then opened and the stroke of I-1 is increased to completion. The pressure in the vessel is increased in this manner until a maximum pressure of 50 Kpsi is reached (usually this limit was on the order of 25-35 Kpsi because of high

---

[1]Models SA-10-10-1.875B-50K and SA-1088-6-.875-200K.

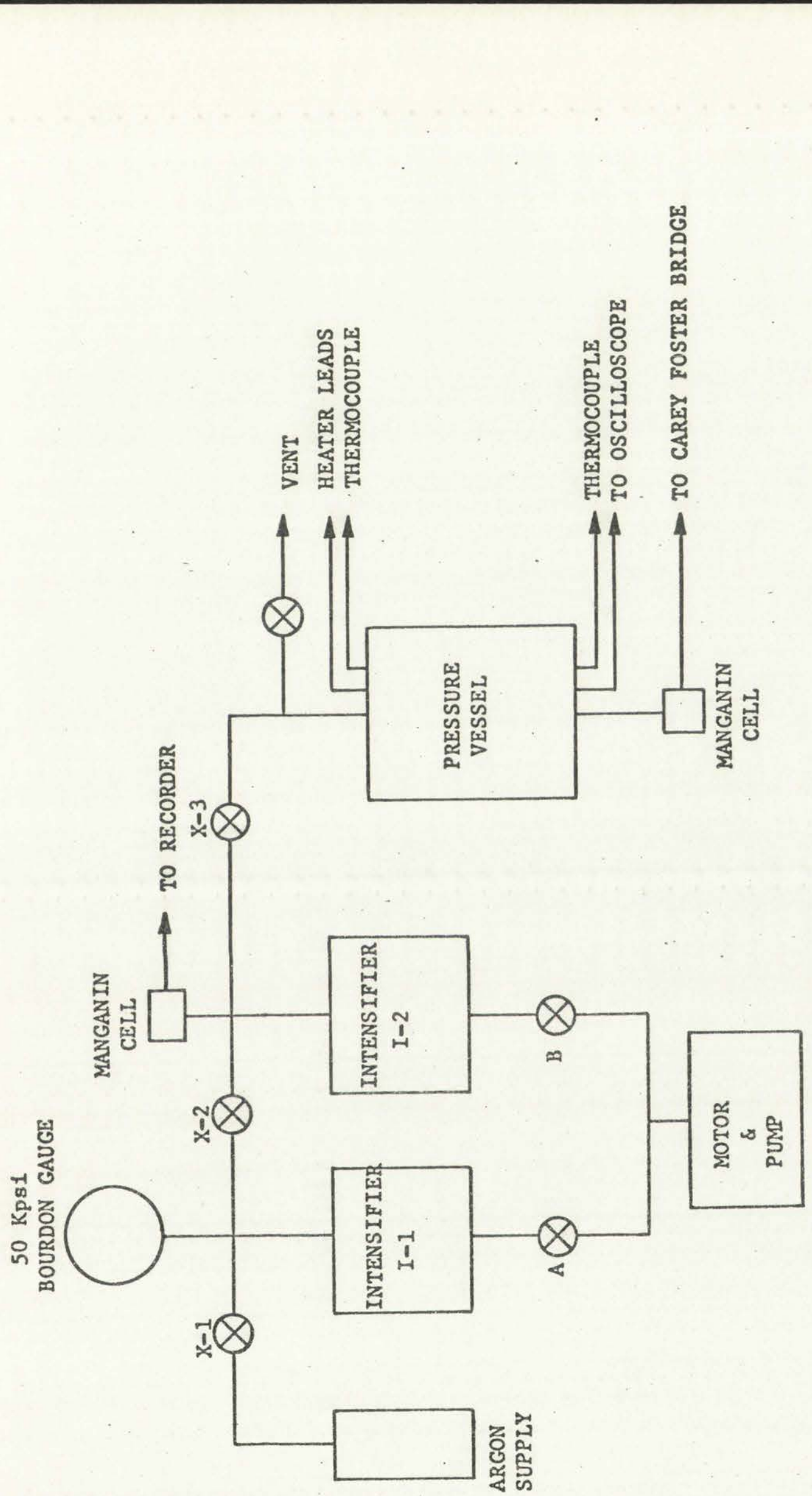

Figure 4. Overall Diagram of the High Pressure System Used in the Experiment

pressure leaks around the packings in the first intensifier). At this point, the second intensifier is run to the top of its stroke with X-2 closed and X-3 opened. X-3 is then closed and the piston in I-2 fully retracted. As before, the first intensifier is used to charge the second to a maximum of 50 Kpsi, so that multiple strokes can be accomplished with I-2.

The rate of stroking of the intensifiers is controlled by a throttle valve in the hydraulic line. Providing that the stroke is not completed, the output of both intensifiers can be controlled with a valve which regulates the pressure in the main hydraulic line. This valve allows fine control of the high pressure side of the intensifier so that any predetermined pressure can be achieved.

The incremental high pressure generated per stroke is dependent upon the compressibility of the gas. For the lower pressures (to about 10-15 Kpsi) the pressure in the vessel was raised about 2-4 Kpsi per stroke of I-1. At pressures on the order of 100-150 Kpsi, a stroke of I-2 would increase the pressure in the vessel by 15-20 Kpsi (for an initial charge of ~ 30 Kpsi).

A bourdon gauge[1] measured the output pressure of I-1 to about a tenth of a percent. A noninductively wound

---

[1]Heise Bourdon Tube Co., Inc., Newtown, Conn.

manganin coil and a recorder[1] were used to continuously monitor the pressure in the second intensifier to approximately 2 percent. A second manganin coil at the vessel allowed the determination of the pressure in the vessel.

Two rupture disks were installed in the line to protect the gauges. A disk set at ~ 2600 psi was installed between X-1 and the bottle supply. Another disk, set at ~ 57 Kpsi was installed between X-1 and X-2 to protect the bourdon gauge.

The pressure vessel was constructed of 4340 heat-treated steel with an 8:1 wall ratio. The inner cavity of the vessel consisted of a nichrome wire wound furnace with an inside diameter of 2 inches and 6 inches in length. A copper-constantan thermocouple was placed near the inside wall of the furnace and the output of this thermocouple was monitored with a silicon controlled rectifier unit.[2] The power supply for the heater was supplied by West Instrument Company. With this unit, the temperature in the vessel could normally be controlled to within $\pm$ 0.1^{o}C.

As shown in the figure, a noninductively wound manganin coil was used to measure the pressure in the

---

[1]Foxboro Dynalog Recorder, Foxboro, Mass.

[2]West Instrument Co., Schiller Park, Ill.

vessel. This coil had been previously seasoned against pressure and temperature, and was calibrated by the manufacturer[1] to within 0.1 percent with a dead-weight tester. The resistance of the coil was measured with a Carey-Foster[2] type bridge and a galvanometer.[3] The bridge was calibrated to read the pressure directly with an error of less than 150 psi over the pressure range employed here.

Two copper-constantan thermocouples,[4] located 180° apart, were used to monitor the temperature of the specimen. These thermocouples were prepared from wire with special limits of error and were accurate to within about 3/8°C over the temperature range used in the present experiment. They were placed in ungrounded stainless steel sheaths 1/16 inch in diameter and a steel cone was brazed to each sheath. Pyrophyllite sleeves were then inserted over the cones for sealing under pressure.

A digital thermometer[5] was used to measure the output of one thermocouple. This instrument displayed the temperature directly and was graduated in 0.05°C steps. The absolute accuracy of the instrument was ~ ± 1.5°C. Although it was not used for any absolute temperature

---

[1]Harwood Engineering Co.

[2]Harwood Engineering Co., Model C.

[3]Honeywell Co., Model 3430, Denver, Colo.

[4]Conax Corporation, Buffalo, New York.

[5]United System Corp., Digitec Model 564, Dayton, Ohio.

measurements, it allowed a convenient record of small temperature changes within the vessel. The millivolt output of the second thermocouple was monitored by a Leeds and Northrup K-3 potentiometer[1] and galvanometer. The potentiometer was calibrated with a standard cell[2] of 1.019141 volts and could be accurately read to 0.5 microvolts. The millivolt readings were converted into temperature with the use of standard tables.[3]

The vessel contained two threaded plugs for access to the cavity. The bottom closure contained the gas inlet port, two heater leads and the control thermocouple. The top closure contained a port for the manganin cell, the two thermocouple leads and four copper leads. The packings for both closures consisted of a brass wedge ring, a lead ring, a teflon ring, a Vitron O-ring, and a brass retaining ring, in that order. The O-ring was placed toward the interior of the vessel and provided the initial seal. The lead ring provided the seal for the intermediate pressure range, and the brass wedge ring provided the seal at the higher pressures.

The sample assembly which is illustrated in Figure 5 was mounted on the top closure. The holder essentially

---

[1]Leeds and Northrup Co., Philadelphia, Pennsylvania.

[2]The Eppley Lab, Inc., Newport, R. I.

[3]National Bureau of Standards Circular No. 561 for Thermocouple Calibration Charts.

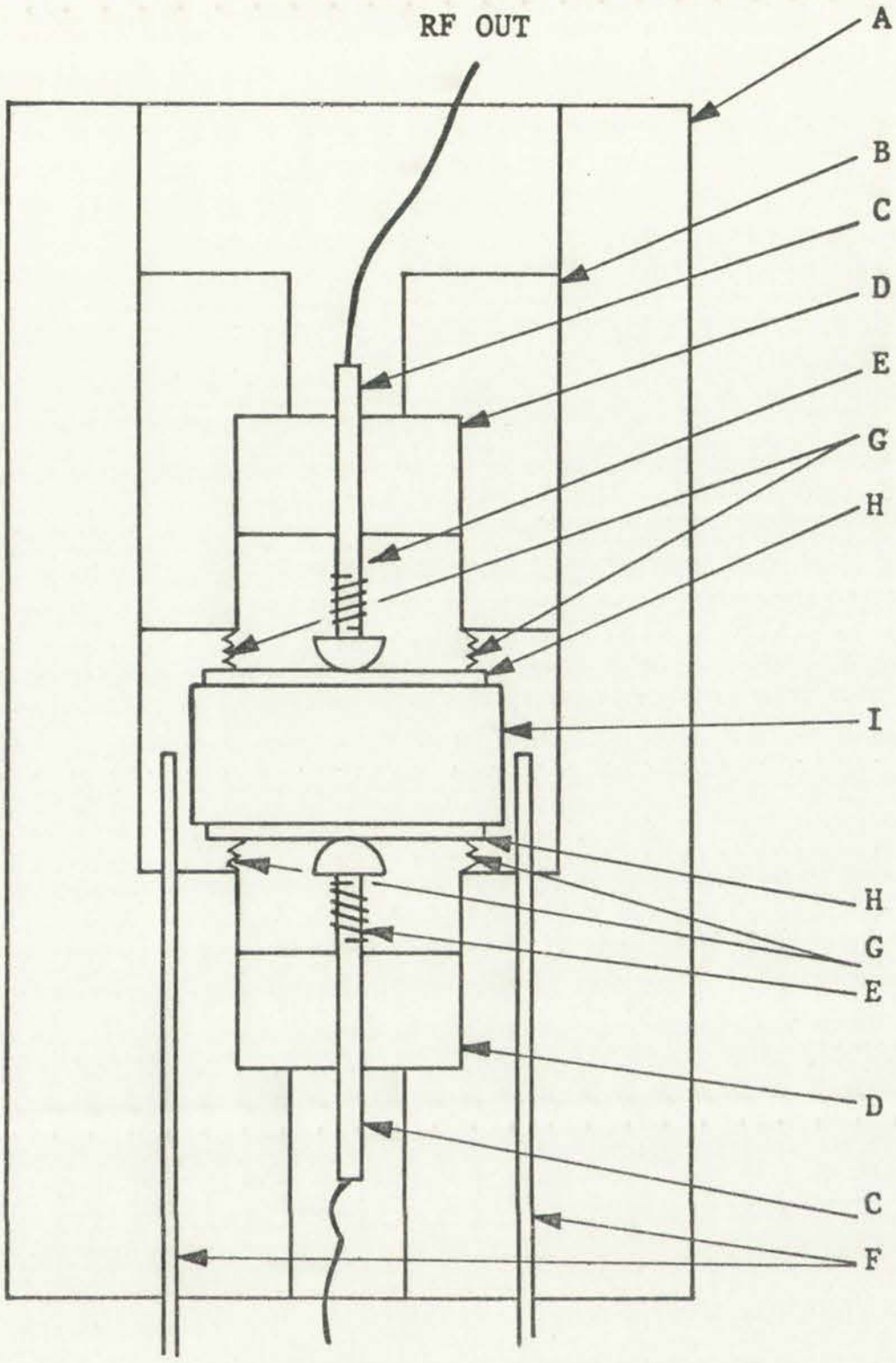

A. ANODIZED ALUMINUM SAMPLE HOLDER
B. ADJUSTABLE ELECTRODE HOLDER
C. COPPER ELECTRODE
D. BORON NITRIDE INSULATOR
E. ELECTRODE SPRING
F. COPPER CONSTANTAN THERMOCOUPLE
G. GROUNDING SPRING TO TRANSDUCER
H. COAXIALLY PLATED TRANSDUCER
I. SAMPLE

Figure 5. Diagram of the Sample Holder Used for the Pressure Measurements

consists of an aluminum cylinder 2 inches in outside diameter and 6 inches in length. The sample and transducer assembly were mounted within the cylinder between the two thermocouples. Two of the copper lead-throughs were connected with copper braid to two spring-loaded copper plungers which provided contact to the active center of the transducers. The other two lead-throughs were tied together and provided ground to the transducer through spring-loaded contact around the outer edge of the transducer. The two RF leads were shielded from each other to reduce feed-through of the signal from the transmitting lead to the receiving lead.

The holder was designed so as to minimize the excess volume in the vessel. This arrangement decreased the pumping time and reduced the safety hazard in the event of a rupture. It was estimated that the net volume in the vessel was about two cubic inches with the holder and specimen in place.

A problem peculiar to the longitudinal measurements was the propagation of longitudinal acoustic vibrations in the argon at the higher pressures. Although the attenuation of sound is extremely high in gases at atmospheric pressure for frequencies in the megacycle range, some propagation in the argon was noted at pressures above about 9,000 psi. This was observed as a late time

arrival which occurred after the echoes in the specimen had attenuated to zero. As the pressure was increased, the amplitude of this signal rapidly increased and the elapsed time from the input pulse decreased. In addition, spurious signals began to form among the echoes in the specimen wave train. To eliminate this effect, fairly fine asbestos cloth was glued to all reflecting surfaces near the specimen in the holder. After this was done, the echo train was completely free of all parasitic signals, with respect to the amplitude of the last observable echo in the specimen. This problem was never observed in the shear measurements.

SECTION III

EXPERIMENTAL RESULTS AND APPLICATIONS

1. Velocity and Attenuation at Atmospheric Pressure

Polymeric materials generally exhibit viscoelastic behavior. That is, the velocities and, consequently, the moduli are frequency dependent. Although this study primarily involves the pressure and temperature dependence of the acoustic velocities, it was considered advisable to estimate the viscoelastic contributions to the elastic moduli. The validity of using the normal relations between the velocities and moduli in various equation of state calculations can then be tested. The approach relies on the determination of the frequency dependence of both the longitudinal and shear velocities and their associated attenuation factors. As shown in Appendix II, the real and imaginary components of the elastic moduli can then be determined. This approach has not been extensively used, primarily because of the difficulty and inherent limitations of making accurate attenuation measurements in high loss materials.

The longitudinal and shear velocities were obtained by immersing the sample assembly in a water bath at 22.2^{o}C. The Williams and Lamb technique was then used to obtain the transit times after the sample had been in

the bath for approximately one hour. Measurements on the specimen were generally taken over a 10 to 15 minute interval.

The attenuation was determined while the specimen was immersed and immediately after the specimen was removed from the bath and dried. This was done to determine whether there was appreciable error due to the transmission of the signal into the water. With the shear measurements, no difference could be detected. This is to be expected since water will not support shear under these conditions. With the longitudinal measurements, however, a constant decrease in the signal of a few db resulted when the specimen was immersed in the water. For this reason, all of the longitudinal attenuation measurements were taken immediately after the specimen had been removed from the bath.

For each frequency, measurements were made on about five to ten specimens and the results averaged. Each specimen was analyzed at least twice to help reduce assembly errors. For the longitudinal measurements, the specimen lengths ranged from 0.37 cm to 1.25 cm. For the shear determinations the range was 0.37 cm to 0.7 cm. The use of various sample thicknesses permitted the detection of systematic errors associated with the velocity and attenuation measurements. However, it was found that no

corrections were required for either the velocity or attenuation data for the frequency range employed here, within the capabilities of the technique (see Appendix I).

Tables 1 and 2 list the results obtained on the longitudinal and shear velocity and attenuation as a function of frequency. The limits of error represent one standard deviation of the mean for the different samples analyzed. The results at 6, 10, and 20 MHz were obtained at the fundamental frequency of the transducer. The data presented at 18 and 30 MHz were obtained at the third harmonic of the crystals.

As shown in Table 1 there is some velocity dispersion in the frequency range of 6-30 MHz (~ 0.4% for both the longitudinal and shear velocities). The observed increase in velocity with frequency is characteristic of a visco-elastic material (13).

There have not been much data reported in the literature as to the velocities and attenuation in polymeric materials in the frequency range used in the present experiment. Gielessen (11) reports longitudinal and shear velocities in PMMA of 2.75 ± 0.03 mm/μsec and 1.37 ± 0.01 mm/μsec, respectively, at 4 MHz and 25°C. Some older work by Hughes et al. (12) lists these velocities as 2.62 mm/μsec and 1.296 mm/μsec at 3.5 MHz and 33°C. Hughes did not report the uncertainties associated

TABLE 1

THE FREQUENCY DEPENDENCE OF THE

LONGITUDINAL AND SHEAR VELOCITY AT 22.2°C

Frequency MHz	Longitudinal Velocity mm/μsec	Shear Velocity mm/μsec
6	2.7564 ± 0.0003	1.4015 ± 0.0009
10	2.7605 ± 0.0005	1.4048 ± 0.0020
18	2.7642 ± 0.0005	1.4051 ± 0.0015
20	2.7651 ± 0.0007	1.4057 ± 0.0007
30	2.7655 ± 0.0003	1.4061 ± 0.0013

TABLE 2

THE FREQUENCY DEPENDENCE OF THE

LONGITUDINAL AND SHEAR ATTENTUATION AT 22.2°C

Frequency MHz	Longitudinal Attenuation db/cm	Shear Attenuation db/cm
6	4.97 ± 0.07	13.64 ± 0.34
10	7.69 ± 0.08	23.99 ± 0.56
18	12.68 ± 0.53	37.21 ± 1.24
20	12.64 ± 0.23	44.28 ± 1.05
30	19.64 ± 0.40	63.94 ± 2.86

with the velocity determinations. However, the technique he used generally allows the determination of the velocity to within a couple of percent.

With respect to attenuation even less is reported in the literature for absorption in this frequency range. Figure 6 illustrates the frequency dependence of the attenuation in nepers per wavelength[1] for both longitudinal and shear waves in PMMA at 22.2°C. Also shown for the longitudinal case are some low frequency results to 1 MHz by Mason (15) and Aubeger (3). No data could be found for the frequency dependence of the shear attenuation. As shown in the figure the attenuation (in nep/λ) is approximately constant at the higher frequencies for both the longitudinal and the shear case. This is consistent with the dependence observed by McSkimin (19) for polyethylene and nylon in the frequency range of 5-40 MHz. At room temperature he also detected a very slight decrease in the constancy of the frequency dependence of the attenuation at the higher frequencies.

With the data presented in Tables 1 and 2, the real parts of the elastic moduli (storage moduli) and the imaginary parts (loss moduli) can be calculated. In principle, all of the moduli can be determined through

---

[1]The attenuation was converted from db/cm to nepers/cm by dividing by 8.686. The conversion to nep/λ was then obtained by multiplying by the propagation velocity and dividing by the frequency at which the measurements were made.

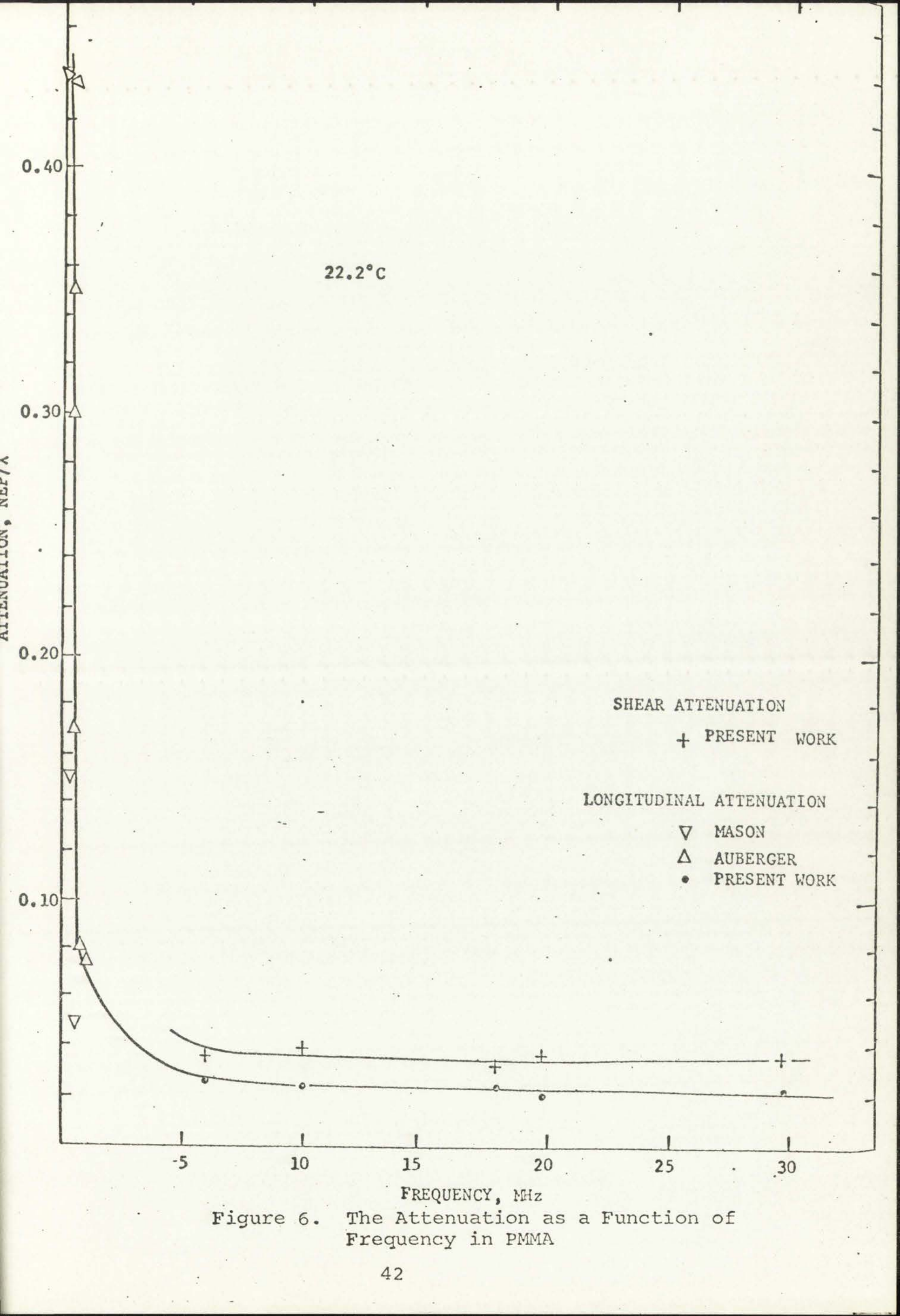

Figure 6. The Attenuation as a Function of Frequency in PMMA

this approach (see Appendix II). However, for most applications to the determination of the equation of state the modulus of primary importance is the bulk modulus, B. It is shown in Appendix II that the real and imaginary components of this quantity can be obtained from the complex components of the longitudinal modulus, L, and the shear modulus, G, as

$$B_1 = L_1 - \frac{4}{3} G_1$$
$$B_2 = L_2 - \frac{4}{3} G_2 \qquad (1)$$

where

$$B^* = B_1 + iB_2$$
$$L^* = L_1 + iL_2$$
$$G^* = G_1 + iG_2$$

The components of L^* and G^* can be obtained from the velocities and attenuations through the relations (see Appendix II)

$$L_1 = \rho V_\ell^2 \frac{(1-\delta_\ell)^2}{(1+\delta_\ell^2)^2}$$

$$L_2 = 2\rho V_\ell^2 \frac{\delta_\ell}{(1+\delta_\ell^2)^2}$$

$$G_1 = \rho V_t^2 \frac{(1-\delta_t)^2}{(1+\delta_t^2)^2}$$

$$G_2 = 2\rho V_t^2 \frac{\delta_t}{(1+\delta_t^2)^2} \qquad (2)$$

where ρ is the density and V_ℓ and V_t are the longitudinal and transverse (shear) velocities, respectively. The quantity δ is defined as $\delta = \frac{\alpha V}{\omega}$ where α is in nep/cm and ω is the angular frequency (δ is equal to α in nep/λ, as given in Figure 6, divided by 2π). The subscripts ℓ or t on δ refer to the longitudinal or shear case, respectively. Since the imaginary parts of the moduli are directly proportional to attenuation, the accuracy with which these quantities can be determined is significantly less than that for the real part where the quantity δ is a small correction factor.

Table 3 shows the frequency dependence of the moduli given in equation (1) at 22.2°C. As shown, the loss part of the longitudinal modulus is less than 1 percent of the real part for all of the frequencies reported here. The imaginary part of the shear modulus is a larger

contribution to the complex modulus, being about 1.2 percent at 6 MHz. However, the imaginary part of the bulk modulus is only about 0.66 percent of the storage part at 6 MHz, decreasing to 0.4 percent at 30 MHz. Hence, for equation of state applications, the high frequency bulk modulus can be calculated from the normal equations of elasticity (assuming δ = 0 in equations 2) to an accuracy of within 1 percent for this range of frequency. For the applications to be discussed later, the elastic moduli were all assumed to be real and were calculated with $\delta = 0$ in equation (2).

Table 3

THE FREQUENCY DEPENDENCE OF THE

COMPLEX ADIABATIC MODULI AT 22.2°C

Frequency MHz	Modulus, dynes/cm^2					
	L_1 X10^{-10}	L_2 X10^{-8}	G_1 X10^{-10}	G_2 X10^{-8}	B_1 X10^{-10}	B_2 X10^{-8}
6	8.965	7.50	2.318	2.71	5.875	3.89
10	8.992	6.99	2.328	2.88	5.887	3.16
18	9.016	6.44	2.330	2.48	5.910	3.13
20	9.022	5.77	2.331	2.66	5.913	2.23
30	9.024	5.99	2.333	2.56	5.914	2.58

2. Temperature and Pressure Measurements

The temperature dependence of the longitudinal and shear velocities was obtained with the Williams and Lamb technique. The samples were previously annealed at a temperature of $\sim 80^{o}C$ for approximately 8 hours. The sample to be studied was then inserted in the vessel and the temperature measurements taken prior to the pressure runs.

As mentioned in Section II, two thermocouples were used to maintain temperature stability to within $\sim 0.1^{o}C$ for a period of at least 15 minutes before measurements were begun. Measurements were then taken over another 10-15 minute period to ensure that the sample had reached temperature equilibrium with the argon.

As explained in Section II and Appendix I, the use of the Williams and Lamb technique requires operation at the resonant frequency of the transducer. Since this is a function of both temperature and pressure, it was necessary to apply this shift in the resonance with environmental changes in order to calculate the transit times. Figure 7 shows the temperature and pressure dependence of the resonant frequencies in X-cut and AC-cut quartz as determined by McSkimin (17,20). He determined the relative resonant frequencies, (f_R/f_{RO}), of these two orientations of quartz over the temperature range of

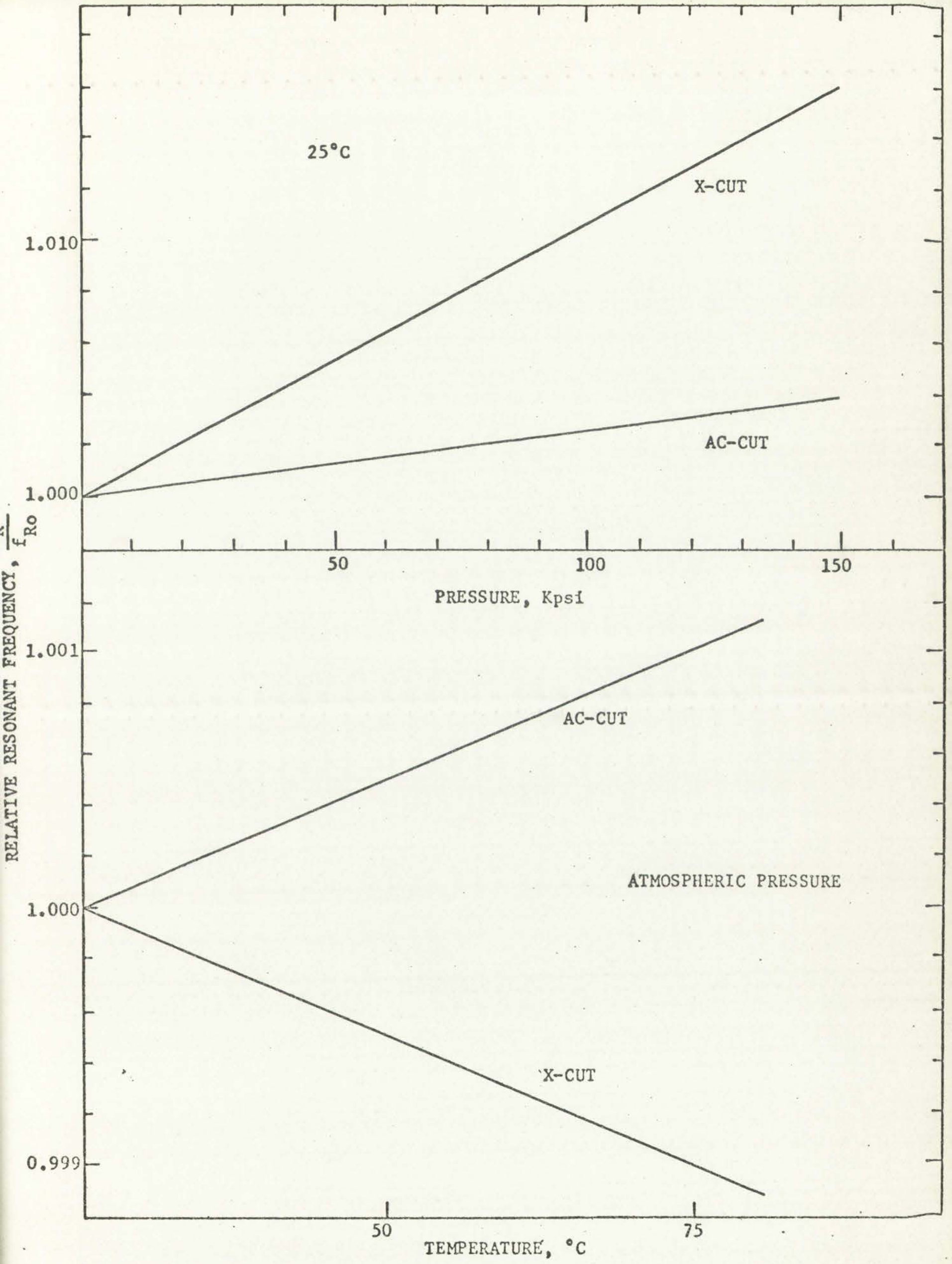

Figure 7. The Relative Change in the Resonant Frequencies of Quartz

-195 to 40°C and from atmospheric pressure to about 32 Kpsi. Since quartz does not exhibit any phase changes over the pressure and temperature ranges employed in the present experiment and since the changes in the resonant frequency were linear, it was felt reliable to extrapolate his results to 75°C and 150 Kpsi. Although this is a rather large range over which to extrapolate, particularly for the pressure range, any errors associated with this technique of extrapolation are felt to be negligible, since the resonant frequency only changes about 1.6 percent for the X-cut quartz and about 0.4 percent for the AC-cut quartz over this range. An error of a few percent in these quantities would constitute an error of only a few hundredths of a percent in the transit time measurements for the sample sizes used here.

Figure 8 shows the temperature dependence of the longitudinal and shear velocities at atmospheric pressure and 6 MHz. The longitudinal measurements were obtained on a specimen ~ 1.35 cm thick. The specimen for the shear measurements was ~ 0.70 cm thick. The experimental data were corrected for thermal expansion (see reference 2) by the relation

$$\ell = \ell_o\left[1 + (6.00 \times 10^{-5})(T-25) + (2.38 \times 10^{-7})(T-25)^2\right]$$

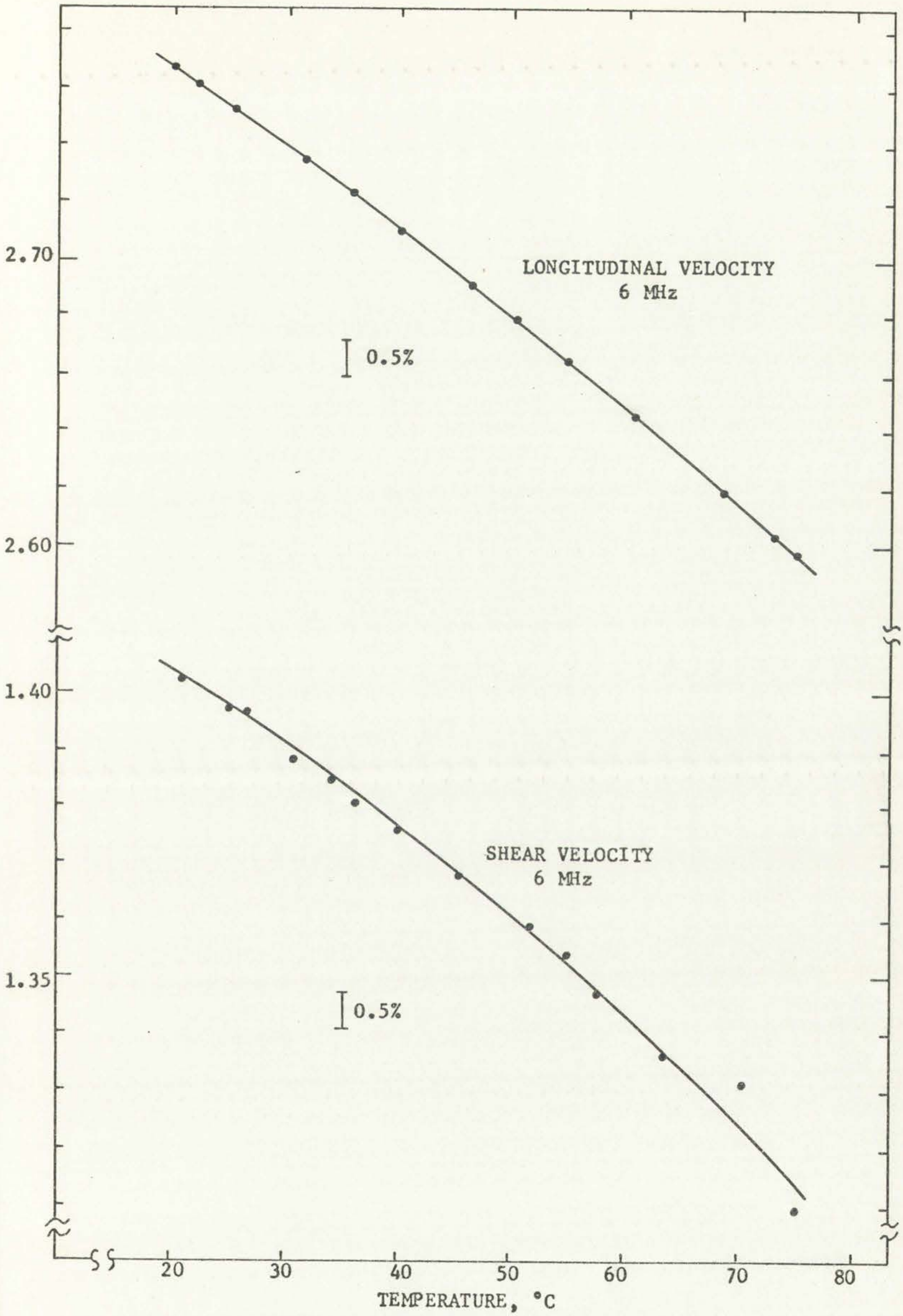

Figure 8. The Longitudinal and Shear Velocities in PMMA as a Function of Temperature at Atmospheric Pressure and 6 MHz

for T in ^{o}C. For the shear velocity, measurements could not be obtained above $\sim 55^{o}$C with the Williams and Lamb technique because of excessive attenuation. For this reason, the measurements between 55^{o}C and 75^{o} were obtained with the transmission technique.

Table 4 lists the values of the longitudinal and shear velocities as a function of temperature in 5^{o}C intervals from 25^{o}C to 75^{o}C as obtained from a least-squares fit of the experimental data. The adiabatic bulk modulus also presented in the table (assumed to be purely real) was calculated from the relation (see Appendix II)

$$B^{s} = L^{s} - \frac{4}{3} G$$

or
$$B^{s} = \rho\left[V_{\ell}^{2} - \frac{4}{3} V_{t}^{2}\right] \qquad (3)$$

The density was obtained from the temperature dependence of the length as presented earlier and given by

$$\rho = 1.18\left[1 + (6.00 \times 10^{-5})(T-25) + (2.38 \times 10^{-7})(T-25)^{2}\right]^{-3}$$

The velocities (in mm/μsec) and the bulk modulus (in dynes/cm^{2}) were fit over the range of 25-75^{o}C by the method of least squares to quadratic equations as follows:

TABLE 4

THE TEMPERATURE DEPENDENCE OF THE

ACOUSTIC VELOCITIES AND THE BULK MODULUS AT

ATMOSPHERIC PRESSURE[a]

Temp. ^{o}C	Longitudinal Velocity mm/μsec	Shear Velocity mm/μsec	Bulk Modulus dynes/cm^{2}x10^{-10}
25	2.7519	1.3977	5.867
30	2.7385	1.3913	5.798
35	2.7246	1.3844	5.733
40	2.7103	1.3771	5.668
45	2.6955	1.3694	5.601
50	2.6803	1.3614	5.534
55	2.6647	1.3529	5.466
60	2.6487	1.3439	5.398
65	2.6322	1.3346	5.329
70	2.6153	1.3249	5.259
75	2.5980	1.3147	5.189

a. The data correspond to a frequency of 6 MHz.

$$V_{\ell} = 2.7519 - (2.647 \times 10^{-3})(T-25) - (8.631 \times 10^{-6})(T-25)^2$$

$$V_t = 1.3977 - (1.2488 \times 10^{-3})(T-25) - (8.207 \times 10^{6})(T-25)^2$$

$$B^s(T) = 5.863 \times 10^{10} - (1.279 \times 10^{8})(T-25) - (1.390 \times 10^{5})(T-25)^2$$

for T in ^{o}C.

Attenuation measurements were also made as a function of temperature in order to evaluate the behavior of the viscoelastic moduli at the higher temperatures. The results are presented near the end of this section and are discussed in relation to the behavior of attenuation with pressure.

As mentioned in the last section the acoustic velocities were first determined as a function of pressure with the transmission technique and with polystyrene fluid as a bond. This was necessary because the echoes within the specimen deteriorated for both the longitudinal and shear measurements at some of the higher pressures. In addition, the amplitude of the wave train commonly exhibited discontinuous jumps at various pressures, and the transducer commonly cracked at room temperature and at the higher pressures.

After various epoxy-based adhesives were tried with little success, a bond material consisting of glycerin and phthalic anhydride was found to provide excellent transmission for both longitudinal and shear wave measurements under pressure. The viscosity of this material could also be controlled by varying the relative amounts of glycerin and phthalic anhydride.

Unfortunately, the author became aware of this bond after all of the isotherms had been determined with the

transmission technique. However, since the Williams and Lamb technique possesses the capability of much higher accuracy, it was thought advisable to repeat all of the previous measurements with the better bond and technique. For the resulting determinations, a ratio of 4:1 of glycerin to phthalic anhydride was used for all of the longitudinal measurements. As previously mentioned, a ratio of 7:4 (glycerin to phthalic anhydride) was used for the shear pressure measurements at 25° and 40°C.[1] A ratio of 1:2 (glycerin to phthalic) was used for these measurements at 55° and 75°C.

For both the longitudinal and shear pressure measurements, the temperature was increased to the desired operating value and a period of approximately one hour or greater allowed for attainment of temperature equilibrium. Measurements were then taken over a 15-20 minute interval at that temperature and atmospheric pressure. For the next measurement, the pressure was increased by approximately 10 Kpsi and a period of about 30 minutes allowed for temperature stabilization to the initial value and equilibrium within the specimen. Four different measurements were then taken over an interval of about 5-10 minutes. Measurements were made in this manner at approximately

---

[1]The higher viscosities resulted in the loss of shear transmission for pressures near 150 Kpsi at room temperature, as in the case of the polystyrene bond.

10 Kpsi intervals over the pressure range of atmosphere to 150 Kpsi. When the maximum pressure was reached, the system pressure was lowered about 25 Kpsi, temperature equilibrium was established and measurements were taken. For decreasing pressure the measurements were typically made in approximately 25 Kpsi intervals to atmospheric pressure. For most isotherms, measurements were made at atmospheric pressure immediately after the pressure run had been completed and again after the sample had remained at atmospheric pressure for about 14-16 hours.

Since the volume and, consequently, the length in PMMA exhibits creep under hydrostatic pressure conditions, it would be expected that the calculated acoustic velocity should be a function of time after the application of pressure. However, it was found that for both the increasing and decreasing pressure runs the acoustic transit time for either the longitudinal or shear measurements was essentially independent of time, within experimental error, for the times associated with the measurements. In a few cases the sample had remained at constant pressure over an hour without a noticeable time effect.[1] In one case, the sample remained at about 15 Kpsi overnight without a noticeable effect.

---

[1]The time effect was difficult to study, since even in the best situations the pressure would decrease a few psi per minute, due to minute leaks in the system at the higher pressures.

For all of the pressure measurements, the relative change in the transit time was initially determined. This was done because of the problem associated with the time dependence of the sample length and because the observed acoustic transit times were essentially independent of time. Figures 9 and 10 illustrate the change in transit time, $\frac{T_o}{T} - 1$, with pressure for the longitudinal and shear velocities in PMMA at 25°C. T_o is the initial transit time and T is the transit time at pressure P. The sample lengths employed for these determinations were 1.3454 cm and 0.6991 cm for the longitudinal and shear measurements, respectively.

Since the velocity is given by $V = \frac{\ell(P)}{T} = \frac{\ell(P)}{T_o} \cdot \frac{T_o}{T}$, it can easily be calculated once the pressure dependence of $\ell(P)$ is known. Also shown in the figures is the pressure dependence of the acoustic velocities for increasing pressure, as calculated through a length relationship given in the next section.

Of particular importance in the figures is the absence of noticeable hysteresis. This is somewhat surprising because of the high compressibility and porosity normally associated with polymers. For the longitudinal measurements the transit time at atmospheric pressure after the sample had been exposed to 150 Kpsi was typically about

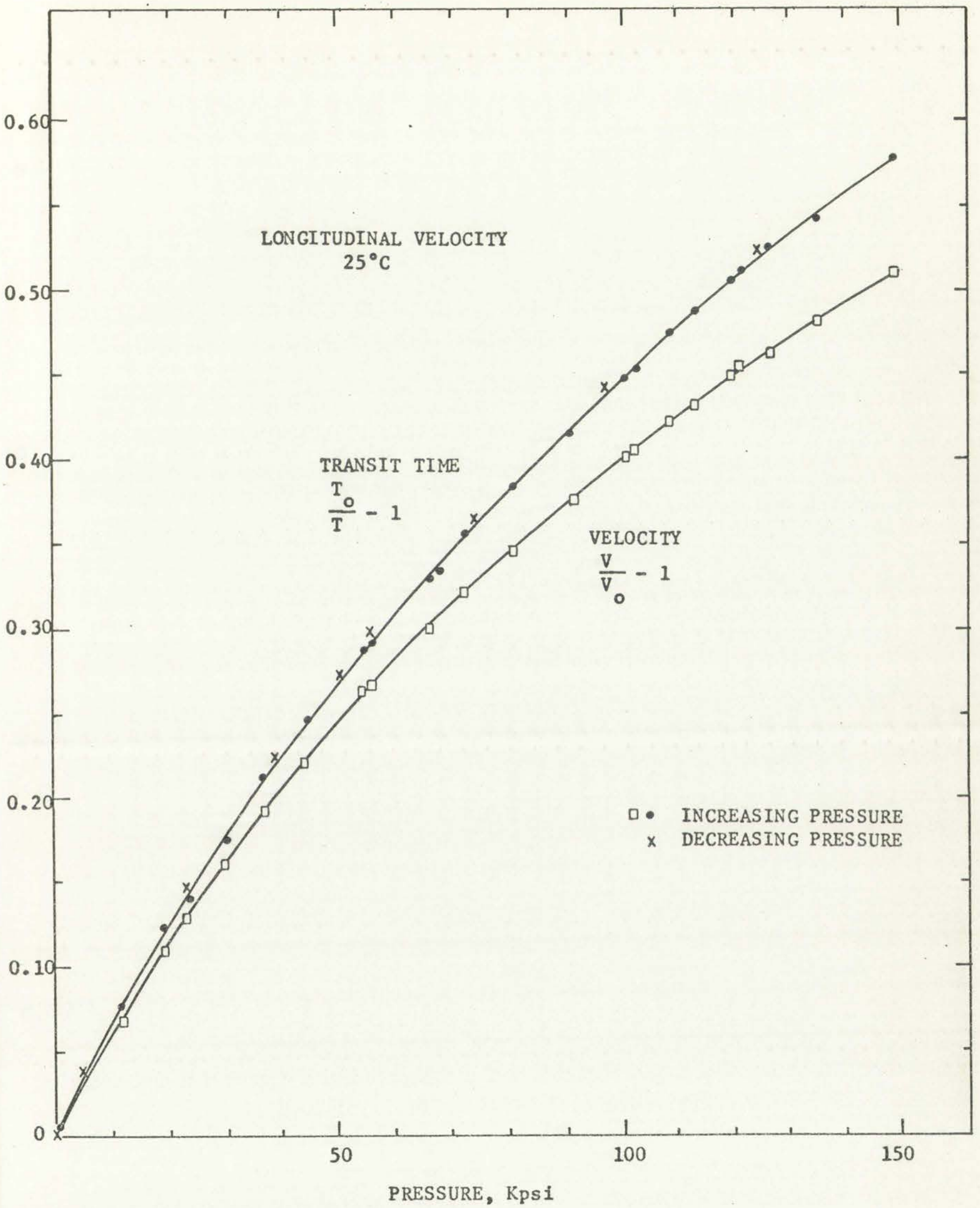

Figure 9. The Relative Change in the Longitudinal Velocity and Transit Time as a Function of Pressure at 25°C. The Acoustic Frequency for these Measurements is 6 MHz

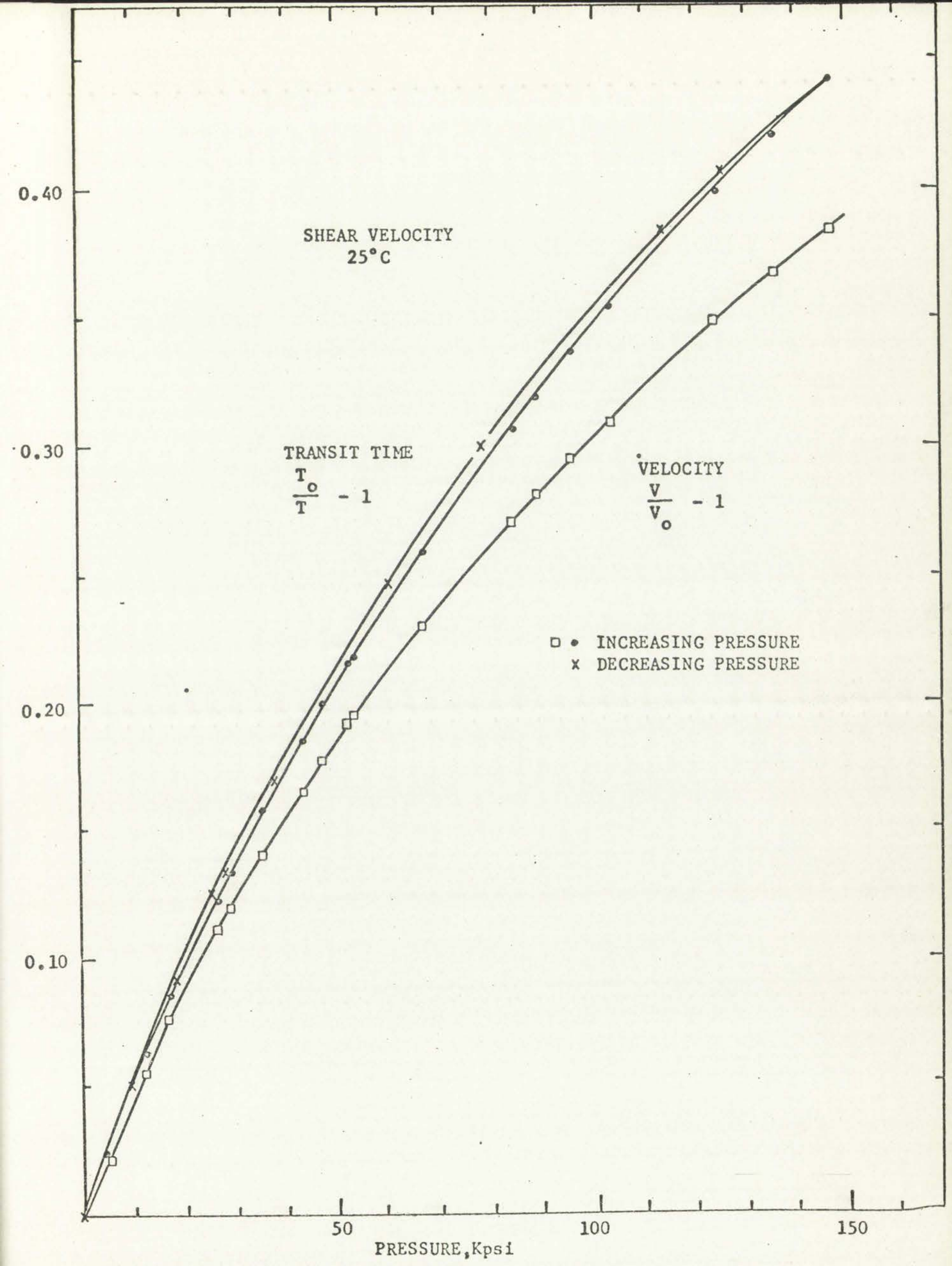

Figure 10. The Relative Change in the Shear Velocity with Pressure at 6 MHz

0.03 percent lower than the original value (at 75°C it was 0.04 percent higher than the original). For the shear measurements, the results obtained at atmospheric pressure after exposure to high pressure were generally about 0.07 percent lower than the original atmospheric results.

Another important factor that is apparent in both figures is the behavior of the results for increasing and decreasing pressure. For the longitudinal case the data corresponding to decreasing pressure are high with respect to those for increasing pressure by a maximum amount of about 0.5 percent near the middle of the pressure range. For the shear measurements the observed difference is a maximum of ~ 0.8 percent at 75 Kpsi. These effects were also present at the higher temperature isotherms for both sets of measurements.

After the pressure runs were completed, the length of the specimen was remeasured. It was found in all cases that the length change after exposure to pressure was less than 0.005 mm. In most cases, the length decreased about 0.002 mm after the pressure and temperature runs.

To evaluate systematic errors in the experiment, two different specimen thicknesses and the two techniques discussed in the last section were used to determine both the longitudinal and shear velocities as a function of pressure. The second set of samples consisted of specimen

thicknesses of 0.8547 cm and 1.4416 cm for the shear and longitudinal measurements respectively. The transit times for both modes were then obtained at 25°C in 20 Kpsi intervals over the complete pressure range. At each pressure, both the Williams and Lamb technique and the transmission method were used to obtain the acoustic transit times. The relative change in transit time as determined by these two methods agreed to within 0.16 percent for the shear measurements and to within 0.1 percent for the longitudinal case. In addition, the relative times agreed to within 0.2 percent of the results obtained on the first set of samples over the complete pressure range. These measurements were not performed for all of the isotherms nor for more sample thicknesses. However, in view of the excellent agreement at 25°C between the two techniques and for two different sample thicknesses, systematic errors are estimated to be less than 0.2 percent for the relative transit times for both the longitudinal and shear velocities.

The later set of measurements with the phthalic anhydride-glycerin bond was also in fair agreement with the earlier measurements using similar specimen thicknesses and with polystyrene fluid as a bond. For the longitudinal data, the agreement between the results for the two different bonds was within 0.5 percent for all of the

isotherms. The agreement for the shear curves was not quite so good. As previously mentioned, the accuracy of the shear measurements at 25°C, and to a certain extent at 40°C, was limited with the polystyrene bond because of loss of signal at the higher pressures. At the lower pressures and for the higher temperature isotherms, the agreement between the results obtained with the different bonds was within 0.3 percent. However, because of the relatively poor quality of polystyrene as a bond material for PMMA, the estimate of systematic errors discussed earlier is assumed to be reliable.

Table 5 lists the coefficients obtained in a least-squares cubic fit of the relative change in transit time as a function of pressure for the different isotherms. The results were obtained for a propagation frequency of 6 MHz and for sample thicknesses of 1.3454 cm and 0.6991 cm for the longitudinal and shear measurements, respectively. For each isotherm the data were fit to an equation of the form

$$\frac{T_o}{T} - 1 = AP + BP^2 + CP^3$$

with P in psi. The limits of error reported in the table correspond to one standard deviation of the mean for the respective coefficients.

TABLE 5

RELATIVE CHANGE IN THE LONGITUDINAL AND SHEAR TRANSIT TIMES AS A FUNCTION OF PRESSURE[a]

Temp. °C		A x 10^6	B x 10^{11}	C x 10^{17}
25.0[b]	L	6.6526 ± 0.0032	-2.9125 ± 0.0066	7.0729 ± 0.0327
	T	5.2678 ± 0.0022	-2.4935 ± 0.0047	6.5329 ± 0.0238
40.0	L	7.1445 ± 0.0046	-3.4668 ± 0.0103	9.3494 ± 0.0547
	T	5.5203 ± 0.0032	-2.5531 ± 0.0069	6.3614 ± 0.0347
55.0	L	7.5704 ± 0.0055	-3.7231 ± 0.0116	9.8458 ± 0.0582
	T	5.8341 ± 0.0025	-2.7765 ± 0.0051	7.0959 ± 0.0245
75.0	L	8.3351 ± 0.0052	-4.3490 ± 0.0108	11.7640 ± 0.0542
	T	6.9376 ± 0.0030	-3.7470 ± 0.0080	10.3550 ± 0.0387

a. The equation used here is $\frac{T_o}{T} - 1 = AP + BP^2 + CP^3$ for pressure in psi.

b. L = longitudinal, T = transverse (shear).

The cubic polynomial approximations were found to fit the experimental data to within about 0.2 - 0.3 percent over the pressure range employed in the experiment. Since this is close to the assumed overall accuracy of the technique, it was felt that it was not appropriate to use a higher order polynomial. The main disadvantage of any non-linear polynomial is associated with the fact that the data cannot be used to extrapolate reliably beyond the measurement region unless the expression can be theoretically justified. This effect will be discussed later with respect

to the continuity of the present results with the high pressure equation of state.

In order to estimate the effect of the visco-elastic contribution to the elastic moduli under different environmental conditions, the relative attenuation at 6 MHz was determined as a function of both temperature and pressure. The attenuation was determined as explained earlier by measuring the amplitude of the echoes in the wave train with an attenuator. For both the longitudinal and shear determinations at the higher temperatures at atmospheric pressure, only the transmitted pulse and one echo could frequently be observed. Hence, for the temperature measurements the accuracy is somewhat reduced. However, for the shear measurements, as many as 4 or 5 echoes could frequently be observed at the higher pressures, so that the accuracy is substantially improved.

Figure 11 illustrates the relative change in attenuation for longitudinal and shear propagation as a function of both temperature and pressure. All of the measurements correspond to a propagation frequency of 6 MHz. For the temperature results at atmospheric pressure, the attenuation is normalized to that at 22°C (α_o = 4.97 and 13.64 for the longitudinal and shear modes, respectively). For the shear measurements above 55°C it was not possible to obtain reliable attenuation results, since one echo could not be obtained.

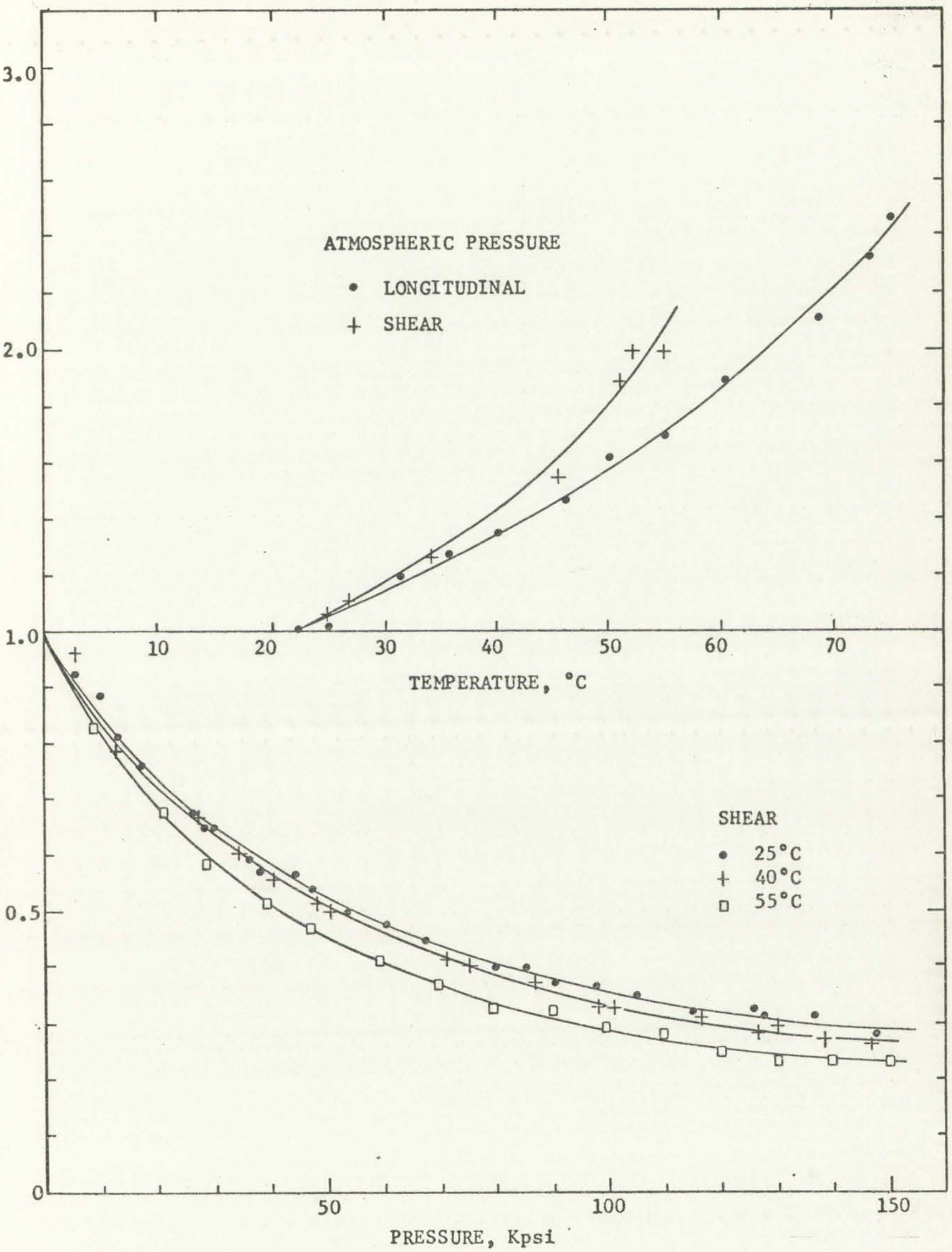

Figure 11. The Relative Change in the Acoustic Attenuation as a Function of Pressure and Temperature

From the longitudinal temperature measurements, it is observed that the attenuation at 75°C is approximately 2-1/2 times that at 22°C. The shear attenuation appears to increase faster with temperature, and is estimated as being approximately three times the room temperature value at 75°C. Since the loss contributions of the complex moduli are directly proportional to attenuation, this implies that the contributions of these moduli are about 2 to 3 times that at 22°C (assuming the velocity and density to be roughly constant). At 22°C the loss contributions to the longitudinal and shear moduli are about 0.8 percent and 1.2 percent of the real parts at 6 MHz, respectively. At 75°C the respective contributions to the longitudinal and shear modulus are therefore about 2 percent and 3-1/2 percent, respectively.

For the shear waves, the attenuation at 150 Kpsi for the first three isotherms is about 1/4 of that at atmospheric pressure, as shown in Figure 11. The variation of the shear attenuation with pressure for the 75°C isotherm was similar to that for the lower temperatures. However, the transmission technique was used for the pressure measurements at 75°C, so that reliable results could not be obtained for the attenuation. The pressure dependence of the shear attenuation implies that the imaginary part of the shear modulus significantly decreases

with respect to the real part at the higher pressures. This implies that with increasing hydrostatic pressure, the shear modulus calculated through the relation $G = \rho V_t^2$ approaches more closely that calculated by ideal elastic theory.

The relative change in the longitudinal attenuation as a function of pressure is not reported in Figure 11 because of the unreliability of determining it at the higher pressures with the present technique. Two main difficulties are associated with this problem. The first results from the loss of acoustic energy at the specimen boundaries as the density of the argon increases. The mechanical impedance (ρV) of the argon rapidly increases with pressure, being approximately equal to the impedance of the specimen at 150 Kpsi. The reflection coefficient for plane wave reflection at the specimen boundary thus decreases so that significant longitudinal wave energy can be lost at specimen boundaries at the higher pressures. The resultant decrease in the amplitude of the reflected echoes is therefore an overestimate of the attenuation in the specimen.

The second problem is probably more appropriate to the difficulties associated with the measurement of the longitudinal attenuation with pressure in the present experiment. It was found that the amplitude of the

reflected echoes within the wave train modulated about 5 db from maximum to minimum intensity at pressure intervals of ~ 30 Kpsi over the range of atmosphere to 150 Kpsi. However, the amplitude of the first transmitted signal changed smoothly with pressure over this interval, increasing about 3 db (from an initial attenuation of 20 db). The oscillation effect in the amplitude of the echoes also appeared to become less pronounced for the higher temperature isotherms. At 75°C the echo amplitude oscillated by an average of approximately 4 db.[1]

This effect is not presently understood. However, one possible explanation relates to the probable visco-elastic behavior of the bond with pressure and temperature. As shown in Appendix I, the bond is assumed to be completely lossless. In addition, it is assumed that the bond completely covers the transducer surface, so that extraneous modes of vibration are not introduced into the system. These assumptions may not be valid at the higher pressures where the viscosity of the bond significantly increases over the initial value and voids can form over the transducer surface because of the difference in compressibilities. The effect did not appear to be present with the polystyrene bond, but the pressure range was

---

[1]Although the period of oscillation was roughly constant in pressure, the magnitude of oscillation generally increased with increasing pressure.

restricted because of the failure of this bond at the higher pressures.[1] In any case, more experimentation will be necessary to study this effect with respect to longitudinal attenuation measurements as a function of pressure.

The modulation effect of the echo amplitude did not appear to influence the velocity determinations. The longitudinal velocity change was found to be smoothly varying with pressure. In addition, as mentioned earlier, there was essential agreement between the velocity determinations for two different sample thicknesses as obtained with both the Williams and Lamb method and the transmission technique.

3. Estimation of the Pressure Dependence of the Strain of the Specimen

The major problem relating to the calculation of the acoustic velocities as a function of pressure in plastics results from the viscoelastic behavior, or time dependence, of the volume under pressure. This effect of volume creep appears to be a general property of polymeric materials, although experimental work in this area is not too extensive with respect to the exact time dependence of the elastic moduli and density variations with pressure. Since

---

[1] With the polystyrene bond, the amplitude of the transmitted signal slightly increased while the echo amplitudes slightly decreased versus pressure. However, both varied smoothly with pressure to ~ 40 Kpsi.

the transit times were determined to within 0.2 percent over the pressure and temperature ranges employed, it was desirable to calculate the length as a function of pressure to this degree of accuracy.

In metals or materials which do not exhibit hydrostatic creep, many experimentalists have used the isothermal compressibility as measured near atmospheric pressure to estimate the length change at constant temperature with pressure. Although this approach is not exact, the compressibilities in many metals are low and a small function of pressure so that the errors introduced into the velocity calculations with this technique are small.[1] Some investigators have extended this approach to plastics. However, for these meterials the determination of the pressure dependence of the length through the use of the atmospheric value of the compressibility is in error; first, because of the large change in the compressibility of plastics at higher pressures and, secondly, because of the time dependence of the length.

Cook (8) has presented a method of calculating the length change from a determination of the transit times of the acoustic velocities with pressure. An outline of his technique corresponding to isotropic symmetry is presented

---

[1]For a metal like aluminum, the total decrease in the length over a pressure range of 150 Kpsi is less than 0.5 percent. An error of 10 percent in the compressibility would constitute an error in the velocity measurements of ~ 0.05 percent.

in Appendix III. Briefly, however, the method consists of using the transit times relating to the longitudinal and shear velocities to calculate the atmospheric value of the adiabatic bulk modulus (reciprocal of the adiabatic compressibility). The conversion to the isothermal bulk modulus[1] is obtained through the appropriate relations (see Appendix III), and the thermodynamic definition of this quantity is then applied to obtain a differential relationship between the volume, or length, and the pressure dependence of the acoustic transit times. With the length ℓ at pressure P defined in terms of the initial length ℓ_o as $\ell = \ell_o/s$, where $s \geq 1$, the resulting equation is

$$s = 1 + \frac{1+\Delta}{3\rho_o} \int_{P_o}^{P} \frac{dP}{\left[V_{o\ell}^2 \left(\frac{T_{o\ell}}{T_\ell}\right)^2 - \frac{4}{3} V_{ot}^2 \left(\frac{T_{ot}}{T_t}\right)^2 \right]} \qquad (4)$$

In this relation, Δ is a correction factor resulting from the conversion to the isothermal bulk modulus, ρ_o is the initial density and $V_{o\ell}$ and V_{ot} are the atmospheric values of the longitudinal and shear velocities, respectively.

---

[1] In estimating length or volume changes with pressure at constant temperature as corresponds to the present experimental conditions, it is necessary to work with the isothermal moduli. The conversion from the adiabatic moduli, as determined ultrasonically, to the isothermal moduli is discussed in Appendixes II and III.

The quantities $\frac{T_o}{T}$ (the subscript refers to the longitudinal or shear case as defined above) are the relative transit times of the acoustic velocities.

In metals the correction factor Δ, which has been assumed to be independent of pressure in equation (4), is small (on the order of 0.05) and the relative transit times are normally linear with pressure. In this case, the use of equation (4), in conjunction with ultrasonic data on the transit times, generally gives length values which are in good agreement with experimental strain measurements as determined, for example, by Bridgman (7). To the author's knowledge, this equation has never been used for plastics, mainly because of the difficulty of determining Δ accurately and because of the nonlinear behavior of the velocities with hydrostatic pressure.

As shown in Appendix III, the correction factor Δ was estimated as 0.346 at 25°C. The initial density and velocities at 25°C were then used in conjunction with the pressure dependence of the relative transit times as given in Table 4 to obtain a numerical result from equation (4) for different pressures.

As previously mentioned, this equation will be somewhat in error because of volume creep. However, it occurred to the author that the use of equation (4) along with high frequency measurements of the bulk modulus should approximate

the initial strain (zero time strain) that would result for the sudden application of hydrostatic pressure (neglecting the temperature effect associated with an adiabatic compression). This approach is of course limited by viscoelastic behavior, of which there is very little information for low frequency in PMMA.

This hypothesis was tested by comparing the results of equation (4) with some recent measurements on hydrostatic creep in plastics by Findley et al. (10). They determined the strain in PMMA over a period of ~ 100 hours at pressures of 1.33, 13.30, 26.60, 40.00 and 50.00 Kpsi. They found that their data fit an equation of the form

$$\epsilon = \epsilon_o + mt^n \qquad (5)$$

where $\epsilon = -\frac{\Delta \ell}{\ell_o}$ is the strain at time t, ϵ_o is a stress-dependent constant corresponding to the instantaneous strain resulting from the application of hydrostatic pressure, m is a stress-dependent function and n is a constant under isothermal conditions. Although Findley could not directly determine ϵ_o because of the rise in temperature associated with the application of pressure, he fit his data to equation (5) by the method of least squares to obtain ϵ_o at the pressures listed above.

Equation (4) was compared with his data by calculating the quantity, $1 - \frac{1}{s} = -\frac{\Delta \ell}{\ell_o}$, at 5 Kpsi intervals to

150 Kpsi and a smooth curve drawn through the results. Figure 12 shows the resulting curve together with Findley's determinations of ϵ_o. As can be seen in the figure, the agreement between the strain as calculated through ultrasonic data and the experimental data of Findley is fairly good to 50 Kpsi. The only other data of the strain with pressure in PMMA that could be found are those by Gielessen and Koppelman (11), which are also plotted in the figure. Their data are consistently higher than Findley's. However, they allowed a 20 minute interval after the application of pressure for temperature equilibrium before making their measurements. If Findley's results on the time dependence of ϵ are applied to their results, there is essentially no difference between the two investigations.

As observed in the figure, the calculated strain appears to be somewhat lower than the experimental data, at least to 70 Kpsi. This could result from a number of causes. The primary factor resulting in the observed difference could arise from the calculation of the correction factor Δ. As shown in Appendix III, this quantity is generally difficult to determine in plastics. An error of 10 percent in this quantity would result in an error of $\sim$ 3 percent in the strain. However, the resulting error in s, and consequently the length, would be $\sim$ 0.06 percent at 50 Kpsi and $\sim$ 0.14 percent at 150 Kpsi.

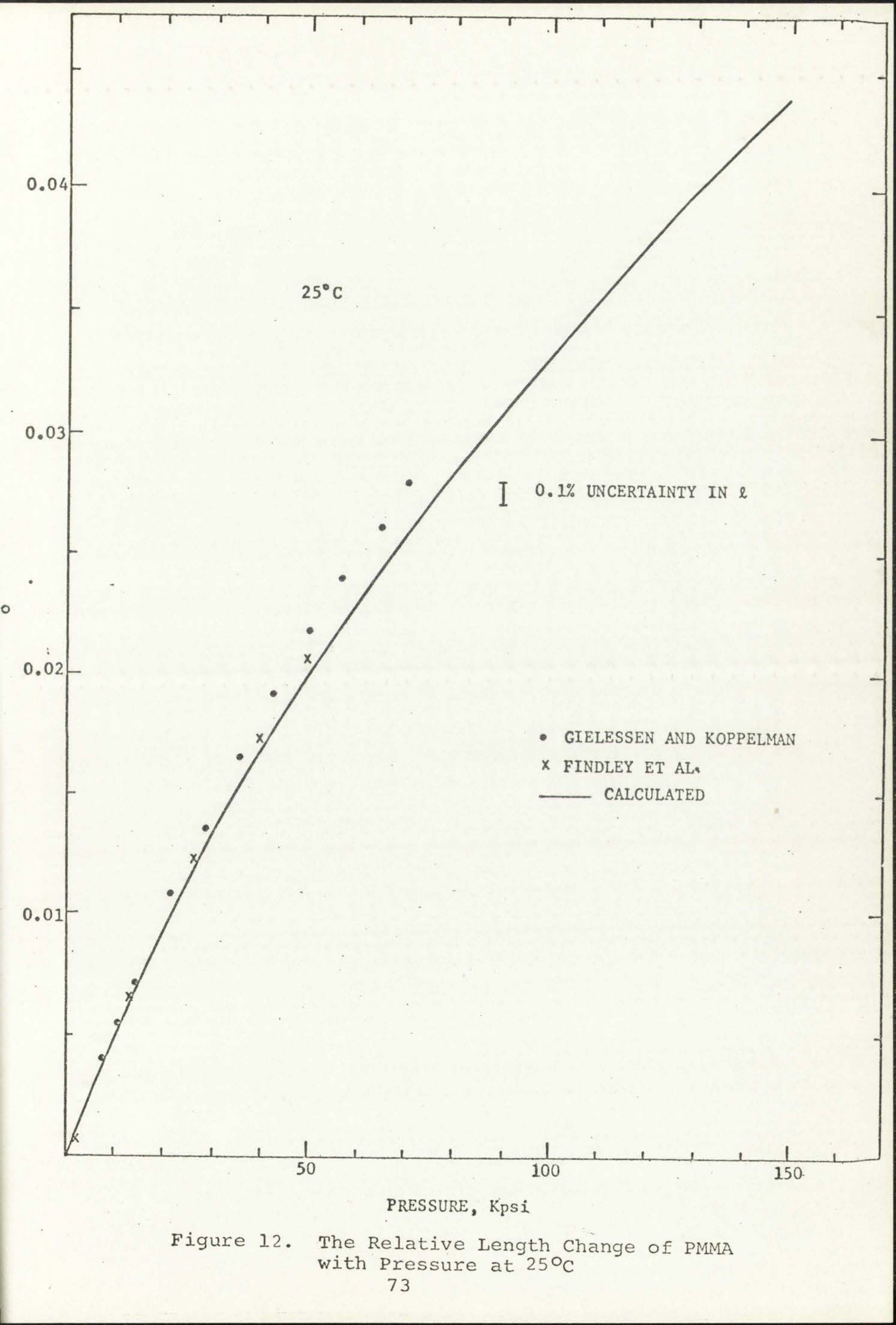

Figure 12. The Relative Length Change of PMMA with Pressure at 25°C

As shown in equation (4), the factor Δ was assumed to be independent of pressure. Δ consists of the volume coefficient of expansion, the Grüneisen ratio (see Appendix III) and the absolute temperature. Of these quantities the Grüneissen ratio and the volume coefficient of expansion are probably slightly pressure dependent so that Δ will be somewhat dependent on pressure. There has not been enough experimental work on the equation of state of plastics to determine reliably the pressure dependence of these quantities at present. However, as illustrated in Figure 12, any pressure dependence of Δ appears to be relatively insignificant in the calculation of s.

Because accurate length determinations in PMMA were not available to 150 Kpsi, the variations of the velocities with pressure were determined with this technique for all of the isotherms. The correction factor as given above is an explicit function of temperature, and was calculated for the various isotherms as 0.413, 0.478 and 0.573 for 40, 55 and 75^{o}C, respectively (see Appendix III). Since s is relative insensitive to uncertainties in Δ, it is estimated that the uncertainty in the length at any pressure and temperature in the present experimental range is within 0.3 percent. Since the density goes as s^3, the uncertainty in the density for the present pressure and temperature ranges is therefore within 0.9 percent.

4. Determination of the Velocities and Bulk Moduli as a Function of Pressure

For each pressure at which the transit time was determined, the true length was calculated by equation (4) and the velocity computed. The velocity data were then fit by the method of least squares to a cubic equation in pressure. Table 6 presents the coefficients of expansion for the relative change in velocity as a function of pressure for the different isotherms studied. The limits of error assigned to the coefficients refer to one standard deviation of the mean.

Figures 9 and 10 illustrate the pressure dependence of the longitudinal and shear velocities in PMMA at 25°C as calculated from the initial strain dependence upon pressure. Also shown in the figures are the resulting least-square fits of the velocities as given in Table 6. The velocities for decreasing pressure are not shown because of the uncertainties in the length for decreasing pressure.

Once the velocities and density are determined as a function of pressure, the pressure dependence of all of the elastic moduli can be calculated. Since the bulk modulus (or the compressibility) is most important for estimations of the volume with pressure, this is the only modulus which is presented here. In Appendix III, it is

TABLE 6

RELATIVE CHANGE IN THE LONGITUDINAL AND SHEAR VELOCITIES AS A FUNCTION OF PRESSURE[a]

Temp. °C		A x 10^6	B x 10^{11}	C x 10^{17}
25.0[b]	L	6.1454 ± 0.0032	-2.8619 ± 0.0065	7.0197 ± 0.0321
	T	4.7627 ± 0.0022	-2.3989 ± 0.0046	6.3399 ± 0.0233
40.0	L	6.5708 ± 0.0045	-3.3818 ± 0.0100	9.2055 ± 0.0532
	T	4.9650 ± 0.0024	-2.4678 ± 0.0052	6.3319 ± 0.0262
55.0	L	6.9469 ± 0.0054	-3.6223 ± 0.0113	9.6610 ± 0.0567
	T	5.2233 ± 0.0024	-2.6365 ± 0.0049	6.7859 ± 0.0237
75.0	L	7.6337 ± 0.0050	-4.2279 ± 0.0106	11.5310 ± 0.0528
	T	6.2458 ± 0.0039	-3.5845 ± 0.0078	9.9866 ± 0.0379

a. The equation used is of the form $\frac{V}{V_o} - 1 = AP + BP^2 + CP^3$ for pressure in psi.

b. L = longitudinal, T = transverse.

shown that the adiabatic bulk modulus is given as a function of pressure and at constant temperature as

$$B^s(P) = \rho_o s\left[V_{o\ell}^2 \left(\frac{T_{o\ell}}{T_\ell}\right)^2 - \frac{4}{3} V_{ot}^2 \left(\frac{T_{ot}}{T_t}\right)^2\right] \qquad (6)$$

where the quantities appearing in this equation have been previously defined. Since an analytical function for s was not found, the relative transit times, the initial velocities and density and the numerical value of s at a given pressure were used to calculate the bulk modulus in 500 psi steps to 150 Kpsi. The resulting values of

$B^s(p)$ were then used to fit a cubic equation in pressure by the method of least squares. Table 7 shows the resulting coefficients and their root mean square deviations

TABLE 7

COEFFICIENTS FOR THE EXPANSION OF THE ADIABATIC BULK MODULUS AS A FUNCTION OF PRESSURE[a]

Temperature, ^oC	$B_o^s(T)$	A_1	A_2	A_3
25.0	58.67	13.543	-0.4188	0.01041
40.0	56.68	14.364	-0.6274	0.02517
55.0	54.66	14.743	-0.6275	0.02258
75.0	51.89	15.081	-0.6630	0.02332

a. $B^s(P,T) = B_o^s(T) + A_1P + A_2P^2 + A_3P^3$. The units of B and P are Kbars.

for the various isotherms. In this case, the expansions are of the form $B^s(P,T) = B_o^s(T) + A_1P + A_2P^2 + A_3P^3$, where the constant $B_o^s(T)$ was not adjusted by the least-squares method, but fixed by the temperature values of the velocities and density at atmospheric pressure. Since the units of B^s and P are pressure, the common unit of Kbar was chosen for both, so that the coefficients given in the table correspond to the pressure and modulus in these units. Table 8 lists the adiabatic bulk modulus in 0.5 Kbar intervals for the different isotherms as determined from these expansions. As shown in the table, the difference

TABLE 8

THE PRESSURE AND TEMPERATURE DEPENDENCE OF THE ADIABATIC BULK MODULUS[a]

Pressure, Kbars[b]	25.0°C	40.0°C	55.0°C	75.0°C
0	58.67	56.68	54.66	51.89
0.5	65.33	63.71	61.88	59.27
1.0	71.79	70.44	68.80	66.33
1.5	78.07	76.90	75.44	73.10
2.0	84.16	83.10	81.82	79.58
2.5	90.07	89.06	87.95	85.81
3.0	95.81	94.80	93.85	91.79
3.5	101.38	100.34	99.54	97.55
4.0	106.79	105.71	105.04	103.09
4.5	112.08	110.90	110.36	108.45
5.0	117.21	115.96	115.51	113.63
5.5	122.21	120.89	120.52	118.65
6.0	127.09	125.71	125.41	123.54
6.5	131.86	130.45	130.18	128.30
7.0	136.51	135.12	134.86	132.96
7.5	141.07	139.74	139.46	137.54
8.0	145.53	144.33	144.01	142.04
8.5	149.91	148.90	148.51	146.49
9.0	154.21	153.49	152.98	150.91
9.5	158.45	158.10	157.45	155.31
10.0	162.62	162.75	161.92	159.71

a. The bulk modulus is given in units of Kbars.

b. Zero pressure corresponds to one atmosphere.

in the modulus for various temperatures appears to decrease as the pressure is increased. At 10 Kbars, the difference between neighboring isotherms is on the order of the experimental uncertainty.

Figure 13 shows the change in the bulk modulus with pressure for the 25°C isotherm. Also shown in the figure is the work of Gielessen and Koppelmann (11) to 71 Kpsi. The agreement between the present study and Gielessen's results is within 2 percent in that range. Gielessen reports an uncertainty in his velocity results of 1 percent, so that the difference between his results and the present data could be as high as 3 to 4 percent.

5. Error Analysis

As mentioned earlier, the null frequencies could easily be determined to within two parts in 10^4. However, systematic errors associated with the measurements of the transit times for different pressure or temperature conditions limit the accuracy with which these quantities can be determined. In general, these errors are hard to estimate. However, since the transit time measurements on two different specimens and with two different techniques agreed to within 0.2 percent with pressure for both the longitudinal and shear measurements, it is felt that the maximum uncertainty of the transit time determinations is 0.2 percent over the pressure range studied in the present experiment.

When the velocities are calculated as a function of pressure, significant error can be introduced through

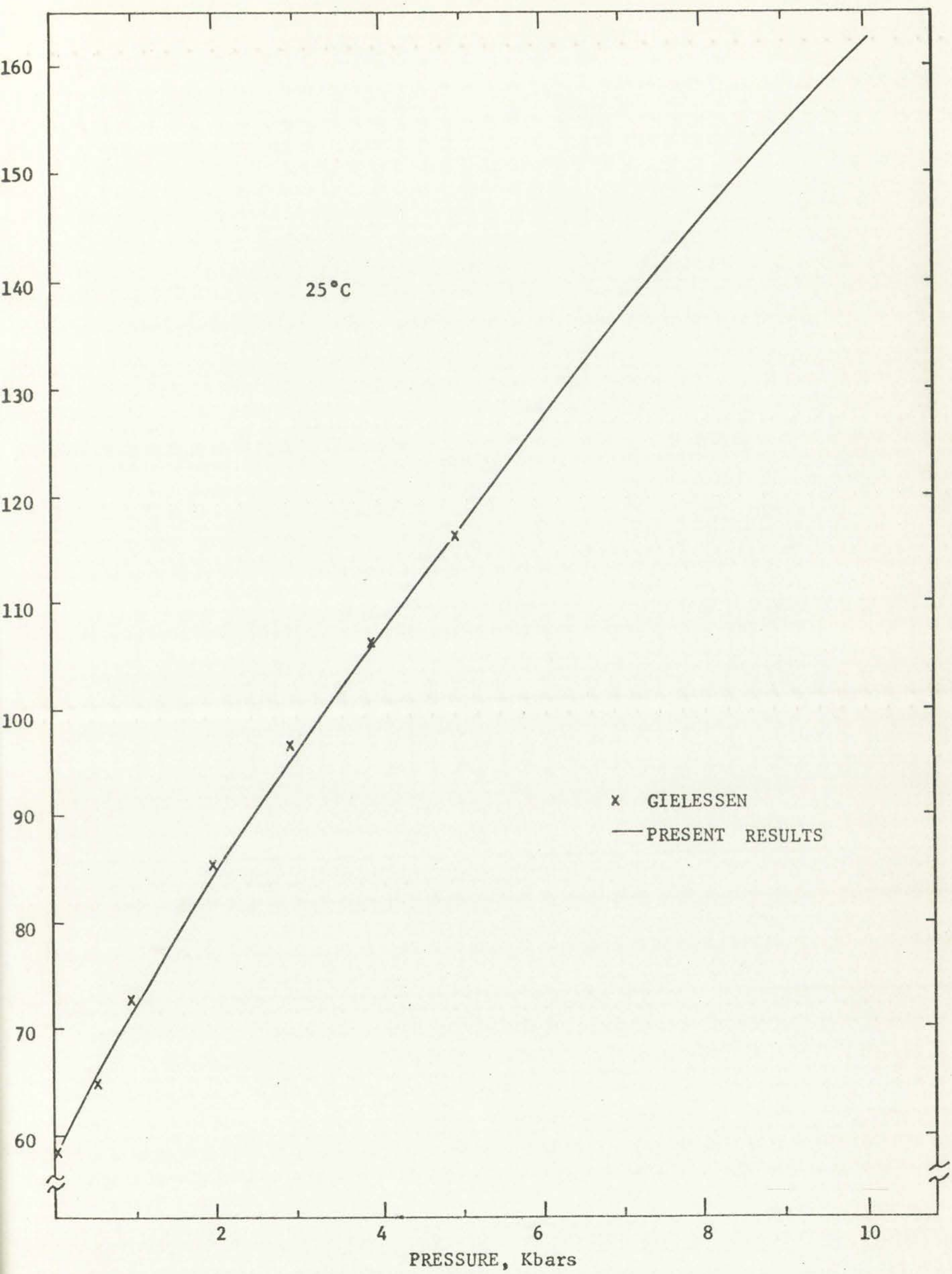

Figure 13. Adiabatic Bulk Modulus as a Function of Pressure

inaccuracies in the estimation of the length under pressure. As previously mentioned, this error should be within 0.3 percent for all of the isotherms, but this estimate relies upon various assumptions which may not be completely valid, particularly at the higher temperatures. In this respect, it would be worthwhile to determine experimentally the length as a function of pressure in PMMA at various temperatures.

In comparison to these two sources of error, the variation of the temperature along a particular isotherm is considered negligible. From the atmospheric pressure results, a temperature change of $1^{o}C$ results in a change of the transit time of $\sim$ 0.1 percent for both the longitudinal and shear measurements. Since the temperature was controlled to within $\pm$ 0.1^{o}C, this source of error should not be a significant factor in the velocity results. Similarly, an uncertainty in pressure of 300 psi will contribute an error of $\sim$ 0.1 percent to the transit time measurements. Since the pressure could be determined to within $\pm$ 150 psi, this contribution to the error in the velocity calculations is $\sim$ 0.05 percent.

If the systematic error is approximated as 0.2 percent, the uncertainty in the length as 0.3 percent and the combined pressure and temperature measurement error as 0.06 percent, the maximum uncertainty in the velocity

determinations is estimated to be on the order of 0.6 percent over the pressure range studied. This result is felt to be conservatively high. The most probable uncertainty, as estimated from the root mean square of the above errors, is ~ 0.35 percent.

The main contributions to the overall uncertainty in the bulk modulus results from the transit time determinations and the factor s (see equation 6).

The errors contributing to the determination of the relative change in the bulk modulus can be obtained by differentiating equation (6) with respect to s, T_ℓ and T_t.[1] If the relative uncertainties in both the longitudinal and transverse transit time determinations are approximated as 0.2 percent, the maximum relative uncertainty in the bulk modulus is estimated to be ~ 1 percent and the root mean uncertainty is 0.65 percent.

As previously mentioned, the uncertainties in the longitudinal and shear velocity at atmospheric pressure and 25°C are estimated to be approximately 0.05 percent and 0.1 percent respectively. From these uncertainties and the standard deviation of 0.1 percent for the density, the most probable uncertainty in the initial adiabatic bulk modulus B_o is estimated to be ~ 0.2 percent.

---

[1] ρ_o, $V_{o\ell}$ and V_{ot} are assumed to be constants for estimating the precision with which the bulk modulus can be determined as a function of pressure.

These estimations relate to the uncertainty in the bulk modulus assuming ideal elastic behavior. Of more fundamental importance, and perhaps a basic limitation, results from the viscoelastic characteristics of the modulus. As shown earlier in this section, B^S is frequency dependent, increasing by about 0.5 percent over the frequency range of 6 to 30 MHz. In addition, the loss part is $\sim$ 0.05 percent of the storage part in this frequency range. These limitations significantly influence attempts to obtain the volume-pressure relationship through this modulus, and further theoretical work is clearly needed to relate the dispersion effect of B^S to the determination of bulk properties of polymers.

SECTION IV

DISCUSSION

1. The Pressure and Temperature Variations of the Velocities and Bulk Modulus

The variation of the acoustic velocities with pressure and temperature as obtained in the present experiment is typical of that exhibited by most solids. That is, the velocities generally decrease with temperature and increase with pressure. In metals, these variations are normally relatively small for the temperature and pressure ranges employed here, so that the derivatives can usually be fit to a linear relation with pressure and temperature. In plastics, this situation is not generally valid, and higher order functions must usually be employed to describe the pressure and temperature dependence of the velocities. As Figures 8, 9 and 10 illustrate, the velocities are definitely not linear in PMMA with respect to either temperature or pressure, for the ranges investigated here.

This nonlinear behavior of the velocities raises a question as to the functional relationship which should be used to fit the experimental data. This is particularly important if the velocities and moduli are to be used to estimate the equation of state outside the range over

which the data are taken. To the author's knowledge, not much theoretical work has been performed in this area, particularly for plastics where the variations are rather large. Soga and Anderson (24) have derived a theoretical relation between the adiabatic bulk modulus and temperature for MgO and $A\ell_2O_3$, which closely fits the experimental data. However, it is not immediately apparent how this relation would apply to the temperature dependence of the acoustic velocities in PMMA.

For the pressure measurements, the problem of choosing a function to fit the experimental data was even greater because of the larger changes in the velocities over the investigated pressure range. The first function that was tried was a quadratic expansion of the form $Y = AP + BP^2$, where Y is the relative change in either the velocities or transit times and P is the pressure. This form did not fit the experimental data very well, being about 1 percent low for the low pressures, about 0.7 percent high for the middle range and about 1 percent low for the highest pressures. This magnitude of variation was thought to be greater than the uncertainty in either the transit time or velocity measurements so that the quadratic was eliminated. A cubic function in pressure was then fit to the data by the method of least squares. In this case, the variation of Y from the experimental data approached the uncertainty

with which the measurements could be obtained so that this form was used to report the data. With the cubic expansion the standard derivation of Y was typically on the order of 0.2 percent.

Three other forms were used to fit the transit time measurements with pressure. The first that was tried was an exponential of the form $Y = A\ (1 - e^{BP})$. The coefficients A and B were found by the method of least squares. This equation gave a standard deviation of Y which was about half that for the quadratic function and slightly higher than that for the cubic function. The equation was then modified by multiplying the above equation by the factor (1 + CP), and the three new coefficients found by least-squares. The standard deviation for this function was slightly less than that for the cubic. One other function of the form $Y = Ae^{B/P}$ was tried. However, this equation gave a standard deviation of about 3 percent.

Since none of these functions could be theoretically justified, it was decided to report the velocity data in terms of a polynomial expansion in pressure. The velocity functions were than used to compute the bulk modulus for small intervals of pressure throughout the pressure range, and these values of the modulus were used to fit a polynomial expansion in pressure. This procedure was necessary

since the longitudinal and shear measurements were not always obtained at the same pressure. I tested the effect that the pressure increment induced into the calculations of the expansion coefficients by choosing the intervals of 500, 1000, 2000 and 3000 psi. For the cubic expansion, the maximum range of the coefficients of A_1, A_2 and A_3 (where $B(P) = B_o + A_1P + A_2P^2 + A_3P^3$) was 0.06 percent, 0.7 percent and 2.5 percent, respectively. For the expansions presented in Table 7, the 500 psi increments were used. Although the coefficients were somewhat influenced by the pressure increments, the bulk modulus calculated at different pressures was relatively insensitive to the data fitting. For the increments noted above, the bulk modulus calculated from the corresponding coefficients agreed to within 0.03 percent for any pressure in the range of atmosphere to 10 Kbars. This is well within the experimental uncertainty associated with this quantity.

In addition to the difficulty of obtaining the functional form of the velocity with pressure from the experimental data, the question arises as to how to fit the bulk modulus as a function of pressure. This is of extreme importance if it is desired to extrapolate the PV relation obtained through this modulus to pressures higher than the measurement range. Anderson (1) has illustrated

that the bulk modulus is linear with pressure for most materials to within the accuracy with which it can be determined. Although this approximation appears to be substantiated by the agreement with the high pressure experimental shock data in some materials, it may not be completely valid for high hydrostatic pressures, particularly for highly compressible materials such as plastics. Physically, it would seem that the volume should approach some limit for the extremely high pressures. This would imply that the bulk modulus should become infinite for infinite pressures. However, this does not predict how the modulus varies with pressure and since it was not known how the bulk modulus should vary in plastics, a cubic expansion was used initially to fit the calculated values. The curve resulting from this expansion fit the calculated values of the adiabatic bulk modulus with a standard deviation of ~ 0.1 percent over the pressure range of atmosphere to 10 Kbars.

Near the conclusion of the present research a two parameter function was found which fit the calculated values of the bulk modulus as a function of pressure slightly better than the three parameter cubic expansion. This equation has the form $B(P) = B_o + A\ell n(1+CP)$, where B_o is the atmospheric value of the bulk modulus and the constants A and C were obtained from a least-squares fit of the data. For the temperatures of 25^oC,

40°C, 55°C and 75°C, the respective values of A were found to be 202.3, 200.5, 184.2 and 173.1 Kbars. The corresponding values of C were 0.0671, 0.0690, 0.0784 and 0.0858 Kbars^{-1} for the respective temperatures of 25°C to 75°C. The physical significance of this relation is not presently understood and further theoretical work is needed to establish its validity in PMMA and possibly other polymers.

2. Estimation of the Equation of State of PMMA

Since this work relates primarily to the experimental determination of the acoustic velocities with pressure in PMMA, this section will not go deeply into the theoretical implications of the data presented here, but rather will discuss the interpretation of the results in terms of a semi-empirical equation that has recently been proposed.

Anderson (1) has suggested that the determination of the acoustic velocities with pressure can be used to define the equation of state of the material under investigation. This, of itself, is not particularly unique, since as was shown in Section III, equation (4) is equivalent to the determination of the isothermal equation of state. As the comparison with experimental strain data illustrated, equation (4) in conjunction with the experimentally determined acoustic transit times can be used to estimate the initial density change as a function of

hydrostatic pressure in PMMA to within ~ 1 percent over the range of atmosphere to 10 Kbars. However, this equation cannot be used to estimate the density for pressures higher than 10 Kbars because of the cubic expansions used for the transit times. In contrast, Anderson's technique relies upon the ultrasonic determination of the pressure dependence of the bulk modulus to extrapolate the volume-pressure relation to pressures beyond the range over which the modulus is determined. The essence of this approach is to determine the adiabatic bulk modulus at atmospheric pressure together with its pressure dependence which, as he has shown, is linear in a great variety of materials. The approach to the determination of the equation of state is then to use the thermodynamic definition of the bulk modulus along with the experimental determination of its pressure dependence as

$$B(P) = - v\left(\frac{\partial P}{\partial v}\right)$$

and

$$B(P) = B_o + B_o'P \ , \qquad (7)$$

where B_o is the atmospheric value of the bulk modulus and B_o' represents its pressure derivative as determined at

atmospheric pressure. Both B_o and B_o' are, in general, functions of temperature, so that a differential relationship can be determined for various temperatures.

Integration of equation (7) between the limits v_o, v, P_o and P yields the volume pressure relation as

$$\frac{v_o}{v} = \left[B_o'\left(\frac{P}{B_o}\right) + 1\right]^{\frac{1}{B_o'}} \tag{8}$$

where the initial pressure P_o has been approximated by zero rather than one atmosphere. Anderson has used equation (8) to estimate the equation of state of several materials to pressures on the order of magnitude of the bulk modulus (~ 500-1000 Kbars in metals), even though ultrasonic measurements to only 3-4 Kbars were used to define B_o and B_o'. He found that if the material did not exhibit any phase changes over the region of interest, the agreement between the extrapolated relation and the actual experimental determination of the high pressure equation of state, such as obtained through shock wave techniques, was remarkably good.

Since his paper, numerous experimental and theoretical investigations have been performed to study the general validity of this approach to various materials. However,

to the author's knowledge, there have not been any attempts to apply this technique to polymeric materials. As shown in the previous section, the application to plastics is limited by viscoelastic behavior, the non-linear relation between the bulk modulus and pressure and the possible presence of transitions. Since no transitions in compressibility measurements to ~ 40 Kbars (7) or in shock measurements to ~ 300 Kbars (26) have been reported for PMMA, it was decided to test the approach with the present data.

Since the bulk modulus is not linear with pressure in PMMA, the exact functional relation between the bulk modulus and the volume derivative of the pressure must be known or equation (7) must be extended to include the higher order terms for the expansion in pressure. The latter procedure is somewhat questionable because of the difficulty in determining the order of the polynomial from experimental data. In addition, equation (7) corresponds to neither purely adiabatic or isothermal quantities, since in ultrasonic experiments the pressure derivative of the adiabatic bulk modulus is determined at constant temperature. It is shown in reference (2) that the pressure derivative of the adiabatic bulk modulus at constant entropy, $B_S^{S'}$, is obtained from the ultrasonically determined quantity, $B_T^{S'}$, as

$$B_s^{s'} = B_T^{s'} + \frac{\gamma T}{B^s}\left(\frac{\partial B^s}{\partial T}\right)_P \qquad (9)$$

where T is the absolute temperature and the other quantities have been previously defined. From temperature measurements of the velocities all of the quantities in equation (9) can be determined, so that the adiabat can be estimated from equation (8) when equation (9) is used to obtain $B_s^{s'}$. When calculating the second adiabatic derivative of the adiabatic bulk modulus, many more terms appear, such as the temperature and pressure derivatives of γ. This quantity is not known very well for plastics (see Appendix III) and there has been no published work, to the author's knowledge, on its pressure and temperature derivatives. For this reason $B_s^{s''}$ cannot be very accurately determined from the ultrasonic measurements.

Because of these difficulties and since the modulus is nearly linear with pressure, it was decided first to estimate the PV relation at 25°C through the use of equations (8) and (9), approximating a linear dependence of the modulus with pressure.[1] The dashed line in Figure 14 shows the adiabat as extrapolated by equation

---

[1]The modulus and its derivatives were obtained at 6 MHz. Since the modulus is frequency dependent, this approach is, at best, only an approximation. However, as shown in Section III, the variation in this modulus over the range of 6-30 MHz is only ~ 0.5% so that the approximation should be fair.

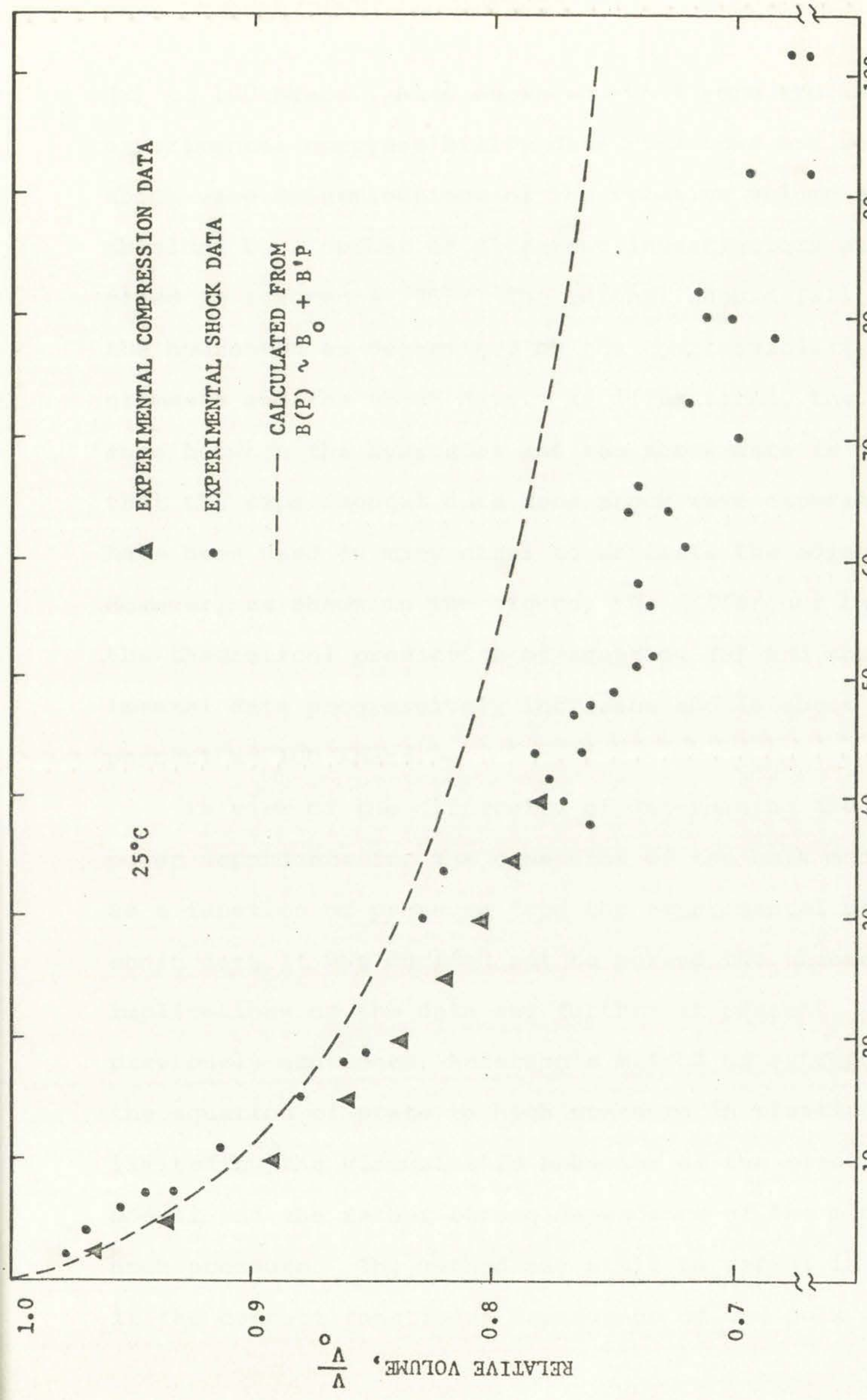

Figure 14. Estimation of the Pressure-Volume Relationship in PMMA to 100 Kbars

(8) to 100 Kbars. Also shown in the figure are some experimental compressibility determinations and some shock wave determinations of the relative volume as obtained by a number of different investigators and compiled in reference (26). The adiabat should fall between the hydrostat as determined by the compressibility measurements and the shock data. As illustrated, the difference between the hydrostat and the shock data is small so that the experimental data from shock wave experiments have been used in many cases to estimate the adiabat. However, as shown in the figure, the difference between the theoretical prediction of equation (8) and the experimental data progressively increases and is about 10 percent at 100 Kbars.

In view of the difficulty of determining the actual power dependence for the expansion of the bulk modulus as a function of pressure from the experimental ultrasonic data, it was decided not to pursue the theoretical implications of the data any further at present. As previously mentioned, Anderson's method of extrapolating the equation of state to high pressure in plastics is limited by the viscoelastic behavior of the elastic moduli and the rather strong dependence of the moduli upon pressure. The method may still be useful in plastics if the correct functional dependence of the bulk modulus

is determined and correction factors, such as the Grüneisen ratio, that have to be applied to the ultrasonic data, are more accurately determined. In any case, the pressure dependence of the ultrasonic velocities in PMMA presented here cannot be used reliably at present to estimate the equation of state above about 10 Kbars.[1]

---

[1]The logarithmic expression presented in the last section was also used to obtain an empirical relation between the volume and pressure. Although this relation gave an extrapolated volume at 100 Kbars which was better than that obtained with the linear approximation, the deviation from the experimental data rapidly increased above 120 Kbars.

SECTION V

CONCLUSIONS AND RECOMMENDATIONS

As has been illustrated, the acoustic velocities can be accurately determined in polymeric materials with the Williams and Lamb technique. This method also allows the precise determination of the pressure and temperature derivatives of the velocities. It was found in the present study that the velocities are nonlinear functions of both the temperature and pressure in the range of 25-75^{o}C and from one atmosphere to 150 Kpsi.

With respect to the pressure measurements, it has been shown that a major contribution to the error in the velocity as a function of pressure results from the uncertainty in the pressure dependence of the length. Although it is felt that the length relation was estimated with a fair degree of accuracy in PMMA, it would be desirable experimentally to determine the length as a function of pressure for the pressure and temperature ranges employed in the present study.

When the elastic properties of PMMA were determined, it was found that the velocities and, consequently, the moduli are slight functions of frequency. From an experimental standpoint, it would be worthwhile to extend the present results to include the measurements of the

(in the absence of phase transitions). However, if these estimations are obtained with the ultrasonic approach, it must be emphasized that the appropriate corrections must be applied to the experimental data in order to estimate the hydrostat or adiabat (2).

It would also be worthwhile to perform ultrasonic pressure measurements on other plastics. This would allow the determination of similarities of the velocities and moduli behavior as a function of pressure and possibly help establish the validity of theoretical or empirical relations of these quantities to pressure and temperature.

APPENDIX I

ANALYSIS OF THE WILLIAMS AND LAMB TECHNIQUE FOR MEASURING ACOUSTIC VELOCITIES

As mentioned in Section I, an ultrasonic wave train is propagated into the specimen from a transmitting transducer. Multiple reflections occur in the specimen, which are detected and converted into electrical signals by the receiving transducer (Figure 2, Section II). A second pulse, phase-coherent with the first, is then applied to the transmitting transducer after an interval of time which corresponds approximately to the round trip time within the specimen. The carrier frequency and the relative amplitudes of the two pulses can be adjusted so that the first transmitted signal from the second pulse interferes with the first echo from the first pulse to give a combined null signal.

Since the envelopes of the RF pulses are essentially flat-topped, continuous wave analysis can be applied to a good approximation. Let the received signal from the second transmitted pulse be given as

$$A \sin \omega t \tag{10}$$

where A is a constant amplitude and $\omega = 2\pi f$, where f is the RF frequency. The first echo from the first transmitted signal arrives at the receiving transducer at a

time t - 2τ relative to the second pulse, where τ is the time delay for one trip through the specimen. The sending and receiving transducers are matched so that the phase shift for reflection from each is given by φ_R. Since the amplitude of the first echo from the first pulse is also A and since it undergoes two reflections (Figure 2, Section II), it may be represented by the relation

$$A \sin[\omega(t-2\tau) + 2\varphi_R] \tag{11}$$

Summing these two equations gives

$$A \{\sin\omega t + \sin[\omega(t-2\tau) + 2\varphi_R]\}$$

$$= 2A \sin[\omega(t-\tau) + \varphi_R]\cos(\omega\tau-\varphi_R) \tag{12}$$

The combined signal may be made zero by varying ω such that

$$\cos(\omega\tau - \varphi_R) = 0 \tag{13}$$

Under this condition

$$\omega\tau - \varphi_R = (2n+1)\pi/2 \tag{14}$$

where n is a positive integer.

In order to evaluate the transit time τ for the corresponding measured value of ω, it is necessary to know the value of n and φ_R. Mason (15) has shown that

the phase shift φ_R can be evaluated by considering the electrical transmission line analog of the acoustic system. He gives the reflection coefficient, R, for a specimen-bonding film-transducer boundary as

$$R = \frac{Z_F' - Z_s}{Z_F' + Z_s} \tag{15}$$

where Z_s is the mechanical impedance of the specimen ($Z_s = \rho_s V_s$) and Z_F' is the equivalent mechanical impedance of the bonding film and transducer as seen from the specimen side. Z_F' is expressed as (17)

$$Z_F' = j\, Z_F \left\{ \frac{Z_T \tan \theta_T + Z_F \tan \theta_F}{Z_F - Z_T \tan \theta_T \tan \theta_F} \right\} \tag{16}$$

where Z_F and Z_T are the impedances of the film and transducer, respectively. θ_T and θ_F are given as

$$\theta_T = \frac{\omega \ell_T}{V_T}$$

$$\theta_F = \frac{\omega \ell_F}{V_F} \tag{17}$$

where ℓ_T and ℓ_F are the thicknesses of the transducer and film, respectively, and V_T and V_F are the corresponding velocities (either shear or longitudinal, depending on the mode under investigation). Williams and Lamb (27) give the reflection coefficient φ_R as

$$\varphi_R = \pi - 2\varphi \tag{18}$$

where $\tan \varphi = \dfrac{|Z_F'|}{Z_s}$

Figure 15 shows the theoretical variation of φ_R for longitudinal waves in a PMMA specimen for values of frequency near resonance and for various bond thicknesses. The curve represents an X-cut quartz transducer ($Z_T = 15.3 \times 10^5$) bonded to the PMMA specimen with a light silicon oil ($Z_F = 1.21 \times 10^5$). The important point about the graph in the figure is that the phase shift is approximately linear for frequencies within a few percent of the resonant frequency. The slope of φ_R as a function of f is also very nearly independent of the bond thickness (and therefore θ_F) for the range given here. Hence, the slope of φ_R near the resonance can be evaluated to a first approximation by assuming $\theta_F = 0$. From equation (18),

$$\varphi_R = \pi - 2 \tan^{-1} \left(\frac{|Z_F'|}{Z_s}\right) \tag{19}$$

For a bond thickness of zero, this becomes

$$\varphi_R = \pi - 2 \tan^{-1}\left[\frac{Z_T \tan \theta_T}{Z_s}\right]$$

or

$$\varphi_R = \pi - 2 \tan^{-1} [K \tan \theta_T] \tag{20}$$

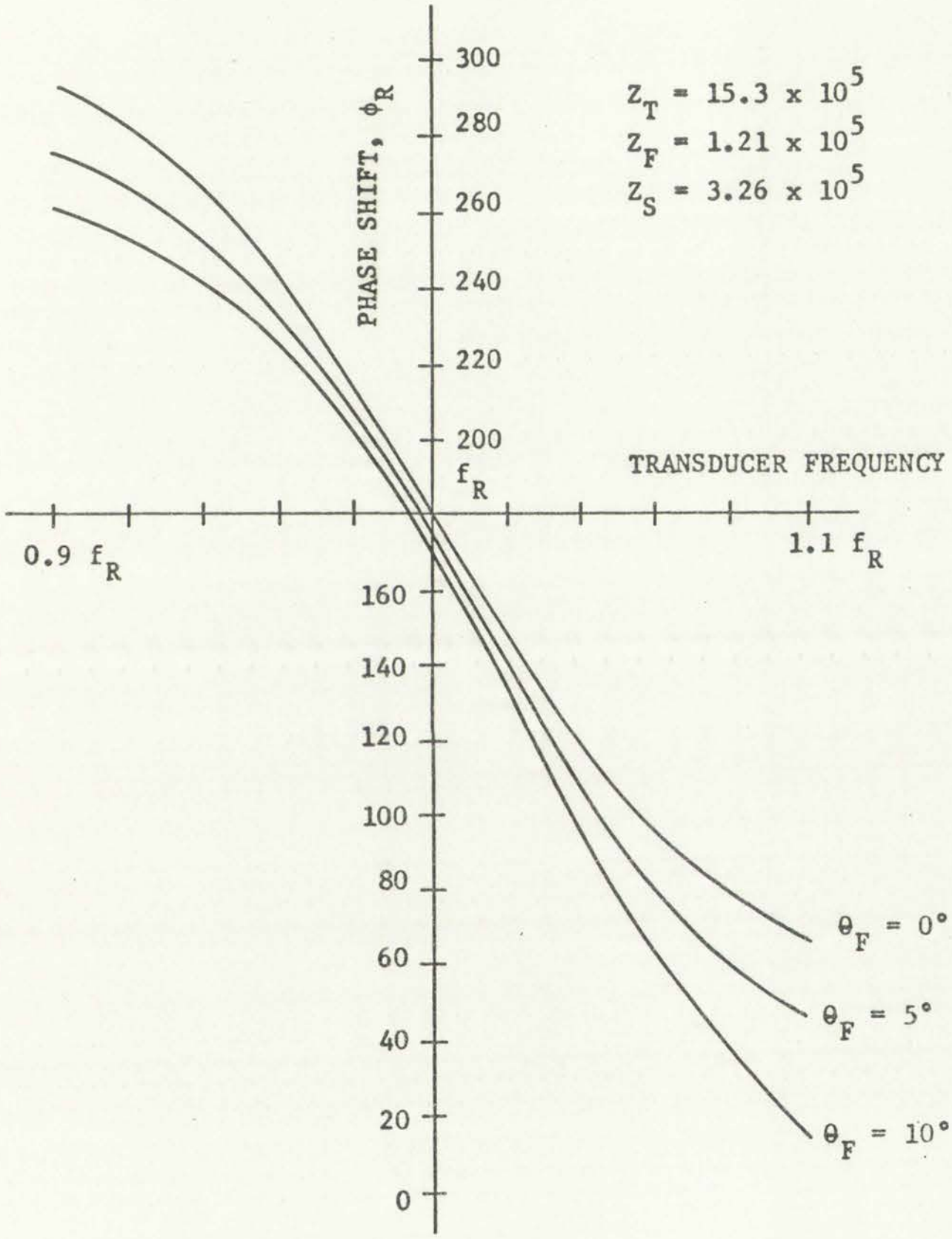

Figure 15. Phase Shift as a Function of Frequency for Acoustic Reflection at the Transducer Boundary

where $K = \frac{Z_T}{Z_s}$. Since $\theta_T = \frac{2\pi f \ell_T}{V_T}$, equation (20) can be written as

$$\varphi_R = \pi - 2 \tan^{-1} \left[K \tan \frac{\pi f}{f_o} \right] \qquad (21)$$

where f_o is the resonant frequency. If equation (21) is differentiated with respect to frequency the following relation is obtained

$$\frac{\partial \varphi_R}{\partial f} = - \frac{2\left[K \frac{\partial}{\partial f} (\tan \pi f/f_o \right]}{1 + K^2 \tan^2 \pi f/f_o}$$

or

$$\frac{\partial \varphi_R}{\partial f} = - \frac{\frac{2K\pi}{f_o} \sec^2 \pi f/f_o}{1 + K^2 \tan^2 \pi f/f_o} \qquad (22)$$

If this is evaluated at the resonant frequency the derivative becomes

$$\left(\frac{\partial \varphi_R}{\partial f}\right)_{f_o} = - \frac{2\pi K}{f_o} \qquad (23)$$

In allowing for the effect of the transducer, Williams and Lamb (27) assume that φ_R can be expanded about resonance, retaining the first expansion term only. That is,

$$\varphi_R \cong \varphi_{Ro} + \left(\frac{\partial \varphi_R}{\partial f}\right)(f - f_o) \qquad (24)$$

Here, φ_{Ro} is the actual phase shift at the transducer-specimen boundary for operation at the resonant frequency of the transducer. If the value of the derivative is substituted into equation (24), φ_R becomes

$$\varphi_R \cong \varphi_{Ro} - \frac{2\pi K}{f_o}(f-f_o) \tag{25}$$

In Figure 15, it is shown that for frequencies near resonance and for θ_F near zero, φ_{Ro} is nearly π. In what follows this will be assumed to be the case. Equation (25) then becomes

$$\varphi_R = \pi\left[1 - \frac{2K}{f_o}(f-f_o)\right] \tag{26}$$

Equation (26) is now substituted into the relation (14) to give the null frequencies in terms of the integer n as

$$2\pi f_n \tau - \pi\left[1 - \frac{2K}{f_o}(f_n-f_o)\right] = \frac{(2n+1)}{2}\pi \tag{27}$$

where f_n corresponds to the nth null frequency. For two frequencies f_n and f_{n+1}, this becomes

$$2f_n\tau - 1 + 2K\left(\frac{f_n-f_o}{f_o}\right) = n + \frac{1}{2}$$

$$2f_{n+1}\tau - 1 + 2K\left(\frac{f_{n+1}-f_o}{f_o}\right) = (n+1) + \frac{1}{2} \tag{28}$$

If the top equation is subtracted from the bottom one, the frequency difference between nulls, $f_{n+1} - f_n$, becomes

$$(f_{n+1}-f_n)2\tau + (f_{n+1}-f_n)\frac{2K}{f_o} = 1 \qquad (29)$$

Therefore, the frequency difference is given in terms of known quantities and the transit time as

$$\Delta f = \frac{1}{2\tau + \frac{2K}{f_o}} \qquad (30)$$

If this is substituted into equation (27), the integer n is given as

$$\frac{f_n}{\Delta f} - 1 - 2K = n + \frac{1}{2} \qquad (31)$$

The value of n can then be determined by measuring frequencies near the resonance of the transducer and substituting into equation (31). To avoid ambiquity in n the ratio of the transducer impedance to the specimen impedance, K, must be known to within 0.25. Once n is known, τ may be determined by substitution into equation (27). The value of τ thus calculated is somewhat in error due to the inaccuracy of K; however, Williams and Lamb (27) illustrate that the true transit time τ_o (neglecting the fact that φ_R differs slightly from π at the transducer resonance) can be obtained by calculating the quantity

$2f_n\tau - 1 = n + \frac{1}{2}$ for values of f_n about resonance. The true transit time, τ_o, is obtained by extrapolating to resonance, since the factor $K\left(\frac{f-f_o}{f_o}\right)$ is then zero. The acoustic velocity in the specimen can consequently be obtained, since $V = \frac{d}{\tau_o}$.

The ultimate accuracy of this approach relies upon the validity of the assumptions involved in the development of equation (27). First, the equation was derived based upon the complex reflection coefficient given earlier. This was derived by Mason (15) for the condition that the transducers are open-circuited at the electrical terminals and that there are no coupling capacitances. This, of course, is not the case in an actual experimental measurement. However, Williams and Lamb (27) made a rather complete study of this effect by varying the air gaps to the electrodes and found that the errors associated with the present experimental condition of the electrode in contact with the transducer introduced an error of less than 0.5 in 10^4. This limitation is therefore considered negligible in the velocity calculations.

Another more important source of error results from the neglect of the coupling film. As shown in Figure 15, a film thickness of 10^o results in a phase shift of 170^o at the resonant frequency, rather than 180^o as assumed

above. At 10 MHz, the resulting error in τ_o would be about 2.5×10^{-3} μsec. For a nominal transit time of 4 μsec the relative error would be about 6 parts in 10^4. Although this is an appreciable error, it is easily corrected for by measuring the velocity in two or more different specimens.

As shown in equation (17), the quantity θ_F is linearly dependent upon the thickness of the bond. This in turn is a function of the flatness of the specimen and somewhat a function of the viscosity of the bond. For the longitudinal measurements at atmospheric pressure, a light silicon oil was applied to the specimen and the transducer was "wrung" on the surface. For constant temperature conditions, the null frequencies could commonly be reproduced to within 3 parts in 10^4 for different assemblies on the same specimen. From equation (17) this implies that θ_F varied by no more than about 5^o from assembly to assembly. It was found in practice that the frequency nulls could be reproduced to within about 100 cps for a given assembly. At 10 MHz this represents an error of 1 part in 10^5, which is therefore a negligible limitation of the technique on plastics.

Diffraction and interaction of the wave with the sample boundaries also lead to sources of error. With respect to the latter consideration, the samples were

prepared with diameters approximately twice the transducer diameter. Samples approximately twice as large as this were used with the same transducers, but no systematic differences were noted. This sample diameter also satisfies the requirement that the sample radius to wavelength ratio (a/λ) be greater than 2.5. Although this requirement is not applicable to shear waves, a general analysis of the Pochhammer-Chree equations representing wave propagation in cylindrical specimens by Tu (25) shows that the pulse velocity undergoes appreciable dispersion for values of a/λ less than ~ 2, approaching the Rayleigh wave surface velocity when this ratio approaches unity, and finally the extensional velocity for $a/\lambda \to 0$. At the lowest frequency used in the present experiment (6 MHz), the ratio of a/λ was on the order of 30 while at 30 MHz it was ~ 150. Therefore, it is considered that for the longitudinal velocity measurements dispersion from geometrical considerations was negligible.

As regards diffraction effects very little experimental or theoretical work has been done, particularly in plastics. However, an empirical study made by McSkimin (18) indicates that if the parameter $\frac{d^{3/2}D^{1/2}}{\lambda^2}$ is greater than 10^4 the measured velocity will be within 0.01 percent of the free space value.[1] In the above formula λ is the wavelength,

[1] The diffraction limited velocity is generally higher than the free space value.

d is the transducer diameter and D is the effective distance traveled by the waves. Since the typical sample thickness was on the order of 10 mm in the present experiment, the above formula gives a value 3.6×10^3 at 10 MHz. According to McSkimin's curve, the measured velocity is then about 0.015 percent high with respect to the free space value.

The diffraction effect can be checked to a certain extent with the Williams and Lamb method. For a given specimen the quantity D is equal to twice the sample thickness when the first echo from the first transmitted pulse is superimposed on the transmitted signal from the second pulse (p = 1). By superimposing the straight-through signal from the second pulse on the second echo from the first pulse (p = 2), the effective propagation distance (now 4 times the sample thickness) is doubled and the above formula gives a result of 1.4×10^4. According to McSkimin the measured velocity should then be about 0.005 percent high, which is a decrease of ~ 0.01 percent from the previous result. This experiment was performed 17 times on different specimens and for different frequencies. Although the p = 2 results were not always lower, the velocities calculated in the two ways agreed on the average to within 0.02 percent (in one case the disagreement was 0.03 percent). For this reason, diffraction is considered to be negligible in the results presented here.

By far, the largest source of error results from the uncertainty in the exact resonant frequency of the transducer. The transducers used for the generation of the acoustic signals were supplied commercially with a quoted frequency uncertainty of 1 percent. Since the Williams and Lamb approach relies upon extrapolation to the resonant frequency, a 1 percent variation in this quantity can result in an error in the velocity of approximately 0.2 percent for the typical sample thicknesses employed here.

If all of the sources of error enumerated above are considered, the worst possible error in the velocity results would be about 0.38 percent. However, for both the shear and longitudinal measurements, the velocities obtained on four to five different specimen thicknesses agreed to within 0.1 percent and 0.05 percent, respectively, when the manufacturer's quoted value for the resonant frequencies was used and a phase shift of 180^{o} for reflection at the transducer boundary was assumed. For this reason, the velocities as obtained with this technique are assumed to be accurate to within 0.05 percent to 0.1 percent.

APPENDIX II

DERIVATION OF THE COMPLEX MODULI FOR MATERIALS OBEYING VISCOELASTIC THEORY

The equations relating to the propagation of acoustic waves in elastic isotropic solids are given in any standard textbook on acoustics. Kolsky (13), in particular, gives an excellent review of the equations of motion in a linear elastic solid and lists all of the elastic moduli in an isotropic solid in terms of the longitudinal and shear velocities. He gives the velocities in terms of the Lamé constants λ and μ as

$$v_\ell = \sqrt{\frac{\lambda+2\mu}{\rho}}$$

$$v_t = \sqrt{\frac{\mu}{\rho}} \qquad (32)$$

Since the generation of small density fluctuations produced by the passage of the wave through the solid is generally assumed to be isentropic, the Lamé constant λ corresponds to the adiabatic modulus. A shear wave does not produce a density change in the solid, so that the isothermal and adiabatic values of μ are identical. Kolsky also gives the relationship of the Lamé constants to the other common elastic moduli in isotropic materials as follows:

Young's Modulus:

$$E = \frac{\mu(3\lambda+2\mu)}{\lambda + \mu}$$

or

$$E = \frac{\rho V_t^2 (3V_\ell^2 - 4V_t^2)}{V_\ell^2 - V_t^2} \tag{33}$$

Shear Modulus:

$$G = \mu$$

or

$$G = \rho V_t^2 \tag{34}$$

Bulk Modulus:

$$B = \lambda + \frac{2}{3}\mu$$

or

$$B = \rho \left[V_\ell^2 - \frac{4}{3} V_t^2 \right] \tag{35}$$

Poisson's Ratio:

$$\sigma = \frac{\lambda}{2(\lambda+\mu)}$$

or

$$\sigma = \frac{V_\ell^2 - 2V_t^2}{2(V_\ell^2 - V_t^2)} \tag{36}$$

Again, with the exception of G, these moduli relate to either the isothermal or adiabatic values. If the moduli

are determined directly from acoustic measurements they generally refer to the adiabatic values.

These results can be extended to a viscoelastic medium by assuming that the propagation constant is related to real and imaginary components as

$$k^* = k_1 - i\alpha \tag{37}$$

where α is an attenuation coefficient in nepers per centimeter. Harmonic waves of the form $e^{i(wt-k^*x)}$ are then attenuated as $e^{-\alpha x}$. The coefficient k_1 is related to the observed phase velocity, V, as $k_1 = \frac{\omega}{V}$. Since k is complex, the complex propagation velocity can be written as

$$V^* = \frac{\omega}{k^*}$$

or

$$V_1 + iV_2 = \frac{\omega}{k_1 - i\alpha} \tag{38}$$

If both the numerator and denominator of equation (38) are multiplied by the complex conjugate of the denominator, the values of V_1 and V_2 become

$$V_1 = \frac{\omega k_1}{k_1^2 + \alpha^2}$$

$$V_2 = \frac{\omega\alpha}{k_1^2 + \alpha^2} \tag{39}$$

These equations can be written as

$$V_1 = \frac{1}{1 + \delta^2} V$$

and

$$V_2 = \frac{\delta}{1 + \delta^2} V \qquad (40)$$

where $\delta = \frac{\alpha V}{\omega}$.

If the effective modulus for wave propagation (either longitudinal or shear) is complex, the relationship between the modulus and velocities are

$$V^* = \sqrt{\frac{M^*}{\rho}}$$

or

$$V^{*2} = \frac{M^*}{\rho} \qquad (41)$$

From the above definitions the real and imaginary components of the modulus become

$$M_1 = \rho \left[V_1^2 - V_2^2 \right]$$

or

$$M_1 = \rho V^2 \left[\frac{1 - \delta^2}{(1+\delta^2)^2} \right] \qquad (42)$$

and $$M_2 = 2\rho V_1 V_2$$

or

$$M_2 = 2\rho V^2 \left[\frac{\delta}{(1+\delta^2)^2} \right] \qquad (43)$$

where M^* of equation (41) has been defined as $M^* = M_1 + iM_2$. From measurements of phase velocity and attenuation, the storage modulus M_1 and the loss modulus M_2 can be obtained for that mode of propagation. For example, for longitudinal propagation the longitudinal modulus is given in terms of the observed phase velocity and attenuation as

$$L^* = (\lambda + 2\mu)^*$$

or

$$L^* = L_1 + iL_2$$

where
$$L_1 = \rho V_\ell^2 \left[\frac{1 - \delta_\ell^2}{(1+\delta_\ell^2)^2}\right] \tag{44}$$

and

$$L_2 = 2\rho V_\ell^2 \left[\frac{\delta_\ell}{(1+\delta_\ell^2)^2}\right]$$

The shear modulus is similarly given as

$$G^* = \mu^*$$

or

$$G^* = G_1 + iG_2$$

where
$$G_1 = \rho V_t^2 \left[\frac{1 - \delta_t^2}{(1+\delta_t^2)^2}\right] \tag{45}$$

and $$G_2 = 2\rho V_t^2 \left[\frac{\delta_t}{(1+\delta_t^2)^2} \right]$$

In principle, all of the other elastic moduli can likewise be determined in terms of L^* and G^*. In particular, the complex bulk modulus, B^*, becomes

$$B^* = \left(\lambda + \frac{2}{3}\mu\right)^*$$

or

$$B^* = L^* - \frac{4}{3} G^*$$

where the individual components are given as

$$B_1 = L_1 - \frac{4}{3} G_1$$

$$B_2 = L_2 - \frac{4}{3} G_2 \qquad (46)$$

These equations apply mostly to polymers, since the viscoelastic attenuation is large enough in some cases to make the loss moduli significant. However, the technique has not received widespread use in the discussion of molecular theories because of the scarcity of velocity and attenuation data over wide ranges of temperature and pressure, although Nolle and Sieck (22) and Marvin and McKinney (14) have used this approach to describe the viscoelastic behavior of various long chain polymers with pressure and temperature.

In applying this method, care must be taken to ensure that the phase velocity is actually determined. If the dispersion is high, this can be a significant experimental problem. In the present experiment, however, the dispersion for both longitudinal and shear propagation in PMMA was found to be only a few tenths of a percent over a frequency range of 6-30 MHz. In addition, pure sine waves of fairly long duration (5-10 μsec) were employed. Thus, it is felt that the velocities determined here closely approximate the phase velocities.

Another potential problem arising in this method results from a possible nonexponential dependence of the attenuation such as would result from diffraction effects. This is easily checked by measuring the amplitude of waves for various propagation distances in the specimen. It was found that the attenuation from one echo to the next was constant within experimental error for PMMA.

APPENDIX III

DERIVATION OF THE LENGTH CHANGE AS A FUNCTION OF PRESSURE IN POLYMETHYLMETHACRYLATE

Cook (8) has presented a method for calculating the length change of a specimen under hydrostatic pressure directly from the measurements of the acoustic velocities as a function of pressure. Although this technique has some reservations with respect to plastics because of viscoelastic behavior, it is presented here since it provides a first approximation of the length of a specimen under pressure.

The length of an isotropic specimen under pressure is assumed to be given as $\ell = \ell_o/s$, where $s > 1$. Since the density is inversely proportional to the cube of the length, it goes as $\rho = \rho_o s^3$, where ρ_o is the density at atmospheric pressure. Both the longitudinal and the shear velocity are represented as

$$V(P) = \frac{\ell(p)}{T(p)}$$

or

$$V(P) = \sqrt{\frac{M(P)}{\rho(P)}} \qquad (47)$$

where M is the effective moculus for propagation (either $\lambda + 2\mu$ or μ) and T is the transit time through the

specimen. From the definitions given above, equation (47) becomes

$$V(P) = \frac{\ell_o}{sT(P)}$$

or

$$M(P) = \frac{\ell_o^2 \rho_o s}{T^2} \tag{48}$$

The adiabatic bulk modulus at any pressure is given as

$$B^s(P) = \rho(P) \left[V_\ell^2(P) - \frac{4}{3} V_t^2(P) \right] \tag{49}$$

whence we obtain[1]

$$B^s(P) = \rho_o \ell_o^2 \, s \left[\frac{1}{T_\ell^2} - \frac{4}{3} \frac{1}{T_t^2} \right] \tag{50}$$

where T_ℓ and T_t are respectively the acoustic transit times for longitudinal and shear waves at pressure P. In terms of the initial velocities and transit times, equation (50) reduces to

$$B^s(P) = \rho_o s \left[V_{o\ell}^2 \left(\frac{T_{o\ell}}{T} \right)^2 - \frac{4}{3} V_{ot}^2 \left(\frac{T_{ot}}{T_t} \right)^2 \right] \tag{51}$$

---

[1]The bulk modulus is also a function of temperature, but this derivation is for constant temperature conditions so that B(P) has been written for simplicity.

The isothermal bulk modulus[1] is given in reference (2) in terms of the adiabatic modulus as

$$B^T(P) = \frac{B^S(P)}{1 + \beta \gamma T}$$

or

$$B^T(P) = \frac{B^S(P)}{1 + \Delta} \tag{52}$$

where β is the volume coefficient of expansion, γ is the Grüneisen ratio and T is the absolute temperature. With respect to pressure P and volume v, the bulk modulus is defined thermodynamically as

$$B^T(P) = -v \left(\frac{\partial P}{\partial v}\right)_T \tag{53}$$

or in terms of the parameter s as

$$B^T(P) = \frac{s(P)}{3} \left(\frac{\partial P}{\partial s}\right)_T \tag{54}$$

If equations (51), (52) and (54) are combined, the relationship between s and P at constant temperature becomes

$$ds = (1 + \Delta) \frac{dP}{3\rho_o \left[V_{o\ell}^2 \left(\frac{T_{o\ell}}{T_\ell}\right)^2 - \frac{4}{3} V_{ot}^2 \left(\frac{T_{ot}}{T_t}\right)^2 \right]} \tag{55}$$

---

[1] It is necessary to use the isothermal bulk modulus for this derivation, since the length of the specimen with hydrostatic pressure must be known for constant temperature conditions as in the present experimental situation.

If the correction factor Δ is assumed to be independent of pressure this reduces to

$$s - 1 = \frac{1 + \Delta}{3\rho_o} \int_{P_o}^{P} \frac{dP}{\left[V_{o\ell}^2 \left(\frac{T_{o\ell}}{T_\ell}\right)^2 - \frac{4}{3} V_{ot}^2 \left(\frac{T_{ot}}{T_t}\right)^2 \right]} \qquad (56)$$

The only unknowns in the above equation are $\frac{T_{o\ell}}{T_\ell}$ and $\frac{T_{ot}}{T_t}$. If these are known as a function of pressure, as in the present experiment, the quantity s can be determined for the range over which the measurements are made.

Since the quantities $\frac{T_{o\ell}}{T_\ell}$ and $\frac{T_{ot}}{T_t}$ are generally linear functions of pressure for metals and the factor Δ is small (on the order of 0.05), the calculated s agrees well with that determined through experimental strain measurements. However, in plastics the quantities $\frac{T_{o\ell}}{T_\ell}$ and $\frac{T_{ot}}{T_t}$ are, in general, not linear functions. In addition, the quantity Δ is considerably more difficult to determine. The main limitation to the calculation of Δ results from the uncertainty in the Grüneisen ratio γ. Although there is a lot of discrepancy in the literature as to the determination of γ, the best estimate of this quantity in PMMA appears to be given in a recent paper by Barker (4). He gives this ratio in terms of the conventional relation

$$\gamma = \frac{\beta B^s}{\rho c_p} \tag{57}$$

where β is the volume coefficient of expansion, ρ is the density and c_p is the specific heat at constant pressure. For polymers, Barker states that only the between-chain vibrational contribution to the specific heat should be used to calculate γ and gives a value of 0.22 j/g^{o}C for c_p in PMMA. This is about an order of magnitude below the calorimetric value. From a density of 1.18 g/cm^3, a volume coefficient[1] of expansion of 2.26×10^{-4}, and a bulk modulus of 5.87×10^{10} dynes/cm^2, a value of 5.13 was calculated for γ. The correction factor, Δ, at 25^{o}C then becomes 0.346.

Since the between-chain contribution to c_p was not known as a function of temperature, γ was assumed to be independent of temperature for these calculations. Although this is a fair approximation, the Grüneisen ratio is generally a slowly decreasing function of temperature. γ was also assumed to be independent of pressure for these calculations.

As shown in Figure 12, Section IV, the agreement between the experimental values of the strain, $-\frac{\Delta \ell}{\ell_o} = 1 - \frac{1}{s}$, and those calculated from equation (56) is fair considering the approximations involved. The experimental points in the figure represent the initial strain after pressure has

[1] β was calculated as an average from references (2), (9) and the Handbook of Chemistry and Physics, 44th Edition.

been applied. In this respect, the measurements of Findley, et al. (10) are considered to be more accurate than those of Gielessen and Koppelmann (11). Gielessen determined the strain at approximately 20 minutes after the application of pressure in order to avoid temperature effects. Findley et al. measured the strain over a period of 100 hours and fit their data to an equation involving the time dependence of the strain.

Although it appears that the approach outlined here might be useful in estimating the length with pressure in polymeric materials, it must be emphasized that experimental determinations of the strain as a function of pressure are necessary to accurately determine the lengths and, consequently, the elastic properties of plastics under pressure.

REFERENCES

1. Anderson, O.L., "The Use of Ultrasonic Measurements Under Modest Pressure to Estimate Compression at High Pressure," J. Phy. Chem. Solids Vol. 27, pp. 547-565, 1966.

2. Asay, J. R. Urzendowski, S. R.,and Guenther, A.H., "Ultrasonic and Thermal Studies of Selected Plastics, Laminated Materials and Metals," Technical Report No. AFWL-TR-67-91, Kirtland AFB, N. Mex., 1968.

3. Auberger, M., and Rinehart, J., "A New Method for Measuring Attenuation of Ultrasonic Longitudinal Waves in Plastics and Rocks," Colorado School of Mines, Internal Report, Golden, Colorado, 1960.

4. Barker, R. E., "Grüneisen Numbers for Polymeric Solids," J. Appl. Phys. Vol. 38, pp. 4234-4242, 1967.

5. Blume, R. J., "Instrument for Continuous High Resolution Measurement of Changes in the Velocity of Ultrasound," Rev. of Sci. Inst. Vol. 34, pp. 1400-1407, 1963.

6. Bridgman, P. W., The Physics of High Pressure, G. Bell and Sons, Ltd., London, 1958.

7. Bridgman, P. W., Collected Experimental Papers, Harvard University Press, Vol. VI, p. 3835, 1964.

8. Cook, R. K., "Variation of Elastic Constants and Static Strains with Hydrostatic Pressure: A Method for Calculation from Ultrasonic Measurements," J. Acoust. Soc. Am. Vol. 29, pp. 445-449, 1956.

9. Corruccini, R. J., and Gniewek, J. J., "Thermal Expansion of Technical Solids at Low Temperatures," NBS Monograph 29, pp. 1-21, 1961.

10. Findley, W. N., Reed, R. M., and Stern, P., Hydrostatic Creep of Solid Plastics," J. Appl. Mech., pp. 895-904, December 1967.

11. Gielessen, J., and Koppelmann, J., "The Pressure Dependence of the Elastic Moduli of Polymethylmethacrylate at Room Temperature," Kolloid Z. Vol. 172, pp. 162-166, 1960.

12. Hughes, D. S., Blankenship, E. B., and Mims, R.L., "Variation of Elastic Moduli and Wave Velocity with Pressure and Temperature in Plastics," J. Appl. Phys. Vol. 21, pp. 294-297, 1949.

13. Kolsky, H., Stress Waves in Solids, Dover Publications, Inc., New York, 1963.

14. Marvin, R. S., and McKinney, J. E., Physical Acoustics, Vol. II, W. P. Mason, Editor, Part B, Chapter 9, Academic Press, New York, 1965.

15. Mason, W. P., Electromechanical Transducers and Wave Filters, D. Van Nostrand Co., Inc., Princeton, 1948.

16. Mason, W. P., Physical Acoustics and the Properties of Solids, Nostrand Co., Inc., Princeton, New Jersey, 1958.

17. McSkimin, H. J., and Andreatch, P., "Analysis of the Pulse Superposition Method for Measuring Ultrasonic Wave Velocities as a Function of Temperature and Pressure," J. Acoust. Soc. of Am. Vol. 34, pp. 609-615, 1962.

18. McSkimin, H. J., "Notes and References for the Measurement of Elastic Moduli by Means of Ultrasonic Waves," J. Acoust. Soc. Am. Vol. 33, pp. 606-615, 1960.

19. McSkimin, H. J., "A Method for Determining the Propagation Constants of Plastics at Ultrasonic Frequencies," J. Acoust. Soc. Am. Vol. 23, pp. 429-434, 1951.

20. McSkimin, H. J., "Elastic Moduli of Silicon vs Hydrostatic Pressure at 25.0° and -195.8°C, J. Appl. Phys. Vol. 35, pp. 2161-2165, 1964.

21. Murnaghan, F. D., Finite Deformation of an Elastic Solid, John Wiley and Sons, Inc., New York, 1951.

22. Nolle, A. W., and Sieck, P. W., "Longitudinal and Transverse Ultrasonic Waves in a Synthetic Rubber," J. Appl. Phys. Vol. 23, pp. 888-894, 1952.

23. Renard, R. B., "Pressure and Temperature Dependence of the Elastic Constants of Ammonium Chloride Near the Lambda Transition," Ph.D. Dissertation, Massachusetts Institute of Technology, 1965.

24. Soga, N., and Anderson, O. L., "The High Temperature Elastic Properties of Polycrystalline MgO and Al_2O_3," Bell Telephone Laboratories, Murray Hill, New Jersey, private communication.

25. Tu, L. Y., Brennan, J. N., and Sauer, J. A., "Dispersion of Ultrasonic Pulse Velocity in Cylindrical Rods," J. Acoust. Soc. Am. Vol. 27, pp. 550-555, 1955.

26. Van Thiel, M., Compendium of Shock Wave Data, Vol. 2 UCRL-50108, Lawrence Radiation Laboratory, Livermore, California, 1966.

27. Williams, J., and Lamb, J., "On the Measurement of Ultrasonic Velocity in Solids," J. Acoust. Soc. Am. Vol. 30, pp. 308-313, 1958.

28. Yarnell, C. F., "The Temperature and Pressure Dependence of the Elastic Constants of Ammonium Bromide," Ph.D. Dissertation, Massachusetts Institute of Technology, 1965.